Impact Factor:						
	ISRA (India)	= **6.317**	**SIS** (USA)	= **0.912**	**ICV** (Poland)	= **6.630**
	ISI (Dubai, UAE)	= **1.582**	**РИНЦ** (Russia)	= **3.939**	**PIF** (India)	= **1.940**
	GIF (Australia)	= **0.564**	**ESJI** (KZ)	= **8.771**	**IBI** (India)	= **4.260**
	JIF	= **1.500**	**SJIF** (Morocco)	= **7.184**	**OAJI** (USA)	= **0.350**

SOI: 1.1/TAS DOI: 10.15863/TAS

International Scientific Journal

Theoretical & Applied Science

p-ISSN: 2308-4944 (print) **e-ISSN:** 2409-0085 (online)

Year: 2022 **Issue:** 05 **Volume:** 109

Published: 12.05.2022 **http://T-Science.org**

Issue **Article**

Denis Chemezov
Vladimir Industrial College
M.Sc.Eng., Corresponding Member of International Academy of Theoretical and Applied Sciences, Lecturer, Russian Federation
https://orcid.org/0000-0002-2747-552X
vic-science@yandex.ru

Ivan Chebryakov
Vladimir Industrial College
Student, Russian Federation

Marina Sergeeva
Vladimir Industrial College
Honorary Worker of Primary Professional Education of the Russian Federation, Master of Industrial Training, Russian Federation

Daria Petrunina
Vladimir Industrial College
Lecturer, Russian Federation

Emil Akhmetov
Vladimir Industrial College
Student, Russian Federation

Vladislav Samoylov
Vladimir Industrial College
Student, Russian Federation

Artyom Gamanistov
Vladimir Industrial College
Student, Russian Federation

REFERENCE DATA OF PRESSURE DISTRIBUTION ON THE SURFACES OF AIRFOILS HAVING THE NAMES BEGINNING WITH THE LETTER H (THE FIRST PART)

Abstract: *The results of the computer calculation of air flow around the airfoils having the names beginning with the letter H are presented in the article. The contours of pressure distribution on the surfaces of the airfoils at the angles of attack of 0, 15 and -15 degrees in conditions of the subsonic airplane flight speed were obtained.*

Key words: *the airfoil, the angle of attack, pressure, the surface.*

Language: *English*

Citation: Chemezov, D., et al. (2022). Reference data of pressure distribution on the surfaces of airfoils having the names beginning with the letter H (the first part). *ISJ Theoretical & Applied Science, 05 (109)*, 201-258.

Soi: http://s-o-i.org/1.1/TAS-05-109-20 ***Doi***: https://dx.doi.org/10.15863/TAS.2022.05.109.20

Scopus ASCC: *1507.*

Introduction

Creating reference materials that determine the most accurate pressure distribution on the airfoils surfaces is an actual task of the airplane aerodynamics.

Materials and methods

The study of air flow around the airfoils was carried out in a two-dimensional formulation by means of the computer calculation in the *Comsol Multiphysics* program. The airfoils in the cross section were taken as objects of research [1-22]. In this work, the airfoils having the names beginning with the letter *H* were adopted. Air flow around the airfoils was carried out at the angles of attack (α) of 0, 15 and -15 degrees. Flight speed of the airplane in each case was subsonic. The airplane flight in the atmosphere was carried out under normal weather conditions. The geometric characteristics of the studied airfoils are presented in the Table 1. The geometric shapes of the airfoils in the cross section are presented in the Table 2.

Table 1. The geometric characteristics of the airfoils.

Airfoil name	Max. thickness	Max. camber	Leading edge radius	Trailing edge thickness
H-6355	6.1% at 15.0% of the chord	5.05% at 40.0% of the chord	0.6824%	0.2%
H-7327	6.8% at 30.0% of the chord	7.4% at 30.0% of the chord	0.8095%	0.9%
HANS6407	6.85% at 20.0% of the chord	6.15% at 40.0% of the chord	0.7646%	0.7%
HAR	10.0% at 30.9% of the chord	0.0% at 0.0% of the chord	0.8482%	0.0%
HAR2	10.0% at 17.0% of the chord	0.01% at 0.1% of the chord	2.8877%	0.0%
HAR3	10.0% at 33.9% of the chord	0.0% at 0.0% of the chord	0.6624%	0.0%
Hatschek	10.0% at 40.0% of the chord	5.0% at 40.0% of the chord	0.9514%	0.0%
HAWKER TEMPEST 37,5% SEMISPAN	14.5% at 37.6% of the chord	1.03% at 39.7% of the chord	1.0736%	0.0%
HAWKER TEMPEST 61% SEMISPAN	11.99% at 38.8% of the chord	0.93% at 40.8% of the chord	0.7444%	0.0%
HAWKER TEMPEST 96,77% SEMISPAN	10.0% at 38.0% of the chord	1.03% at 40.1% of the chord	0.5025%	0.0%
HD45	7.5% at 28.2% of the chord	1.4% at 37.7% of the chord	0.5712%	0.0%
HD46	7.0% at 26.4% of the chord	1.4% at 37.8% of the chord	0.553%	0.0%
HD47	6.5% at 26.6% of the chord	1.39% at 38.0% of the chord	0.5234%	0.0%
HD48	8.0% at 27.2% of the chord	2.5% at 42.6% of the chord	0.6361%	0.0%
HD48A	8.5% at 28.6% of the chord	2.5% at 42.3% of the chord	0.6981%	0.0%
HD48B	9.0% at 28.2% of the chord	2.3% at 41.9% of the chord	0.7646%	0.0%
HD50	8.0% at 26.0% of the chord	1.3% at 29.9% of the chord	0.8086%	0.0%
HD53	7.5% at 24.8% of the chord	1.2% at 30.6% of the chord	0.7049%	0.0%
HD54	7.0% at 24.3% of the chord	1.4% at 30.0% of the chord	0.6044%	0.0%
HD800	8.0% at 30.3% of the chord	0.14% at 0.0% of the chord	0.5781%	0.0%
HD801	7.0% at 30.9% of the chord	0.14% at 0.0% of the chord	0.5433%	0.0%
HE82R1-6	8.33% at 25.0% of the chord	6.34% at 45.0% of the chord	1.4517%	0.35%
Hill SR 2	13.7% at 30.1% of the chord	6.85% at 20.0% of the chord	1.0525%	0.0%
HILL-SR2	13.6% at 30.0% of the chord	6.9% at 30.0% of the chord	1.0525%	0.0%
HL 73-6508	7.9% at 40.0% of the chord	5.35% at 50.0% of the chord	0.7345%	0.25%
HL 74-3512	11.9% at 40.0% of the chord	2.7% at 50.0% of the chord	0.7862%	0.2%
HL 74-5508	7.8% at 40.0% of the chord	3.9% at 40.0% of the chord	0.5828%	0.2%
HL 75-5414	14.4% at 40.0% of the chord	5.54% at 40.0% of the chord	1.1155%	0.1%
HL 75-K-3308	8.03% at 40.0% of the chord	4.01% at 40.0% of the chord	0.6275%	0.25%
HL 80-13353	13.4% at 30.0% of the chord	3.15% at 30.0% of the chord	1.1886%	0.1%
HL743512	11.9% at 40.0% of the chord	2.7% at 50.0% of the chord	0.7862%	0.2%
HL813353	13.45% at 30.0% of the chord	3.17% at 30.0% of the chord	1.1898%	0.1%
HN 380	9.15% at 31.6% of the chord	2.33% at 46.9% of the chord	0.6286%	0.0%
HN-003	10.84% at 31.6% of the chord	2.44% at 46.9% of the chord	0.7959%	0.0%
HN-032	7.83% at 28.7% of the chord	1.74% at 46.9% of the chord	0.5471%	0.0%
HN-033	8.05% at 28.7% of the chord	1.85% at 46.9% of the chord	0.5724%	0.0%
HN-034	8.05% at 31.6% of the chord	1.85% at 46.9% of the chord	0.4503%	0.0%
HN-035	8.05% at 28.7% of the chord	1.85% at 46.9% of the chord	0.5318%	0.0%
HN-036	7.85% at 28.7% of the chord	1.65% at 46.9% of the chord	0.5107%	0.0%
HN-038	8.05% at 31.6% of the chord	1.85% at 46.9% of the chord	0.4634%	0.0%
HN-1023	10.2% at 31.6% of the chord	2.38% at 46.9% of the chord	0.711%	0.0%
HN-1027	7.5% at 31.6% of the chord	2.55% at 46.9% of the chord	0.4284%	0.0%
HN-1029	8.06% at 28.7% of the chord	2.21% at 46.9% of the chord	0.5121%	0.0%
HN-1033	7.85% at 28.7% of the chord	2.47% at 43.7% of the chord	0.5203%	0.0%
HN-1033A	7.55% at 28.7% of the chord	2.15% at 43.7% of the chord	0.4917%	0.0%
HN-1036	8.54% at 28.7% of the chord	1.83% at 43.7% of the chord	0.572%	0.0%
HN-1038	8.14% at 28.7% of the chord	1.52% at 43.7% of the chord	0.5299%	0.0%
HN-1051	8.55% at 28.7% of the chord	2.0% at 50.0% of the chord	0.6137%	0.0%

HN-1054	8.55% at 28.7% of the chord	1.65% at 46.9% of the chord	0.587%	0.0%
HN-1070	6.55% at 25.9% of the chord	1.74% at 43.7% of the chord	0.4334%	0.0254%
HN-153S	8.34% at 28.7% of the chord	0.0% at 0.0% of the chord	0.5507%	0.0%
HN-163	8.55% at 31.6% of the chord	1.78% at 43.7% of the chord	0.5297%	0.0%
HN-163TA	8.65% at 31.6% of the chord	1.65% at 43.7% of the chord	0.541%	0.0%
HN-163TB	8.35% at 31.6% of the chord	1.85% at 43.7% of the chord	0.5096%	0.0%
HN-184	8.55% at 31.6% of the chord	1.78% at 46.9% of the chord	0.5264%	0.0%
HN-184M	8.55% at 31.6% of the chord	2.38% at 46.9% of the chord	0.5236%	0.0%
HN-188	10.38% at 31.6% of the chord	2.38% at 46.9% of the chord	0.7573%	0.0%
HN-203	10.8% at 31.6% of the chord	2.34% at 43.7% of the chord	0.7077%	0.0%
HN-211	8.14% at 31.6% of the chord	1.65% at 46.9% of the chord	0.4997%	0.0%
HN-216	8.08% at 31.6% of the chord	1.94% at 43.7% of the chord	0.4905%	0.0%
HN-216TA	8.25% at 31.6% of the chord	1.78% at 43.7% of the chord	0.5071%	0.0%
HN-217	8.08% at 31.6% of the chord	2.34% at 43.7% of the chord	0.4827%	0.0%
HN-227	8.99% at 31.6% of the chord	2.35% at 46.9% of the chord	0.5287%	0.0%
HN-239	8.12% at 31.6% of the chord	2.14% at 46.9% of the chord	0.4835%	0.0%
HN-274S	9.14% at 25.9% of the chord	0.0% at 0.0% of the chord	0.584%	0.0%
HN-275S	10.27% at 25.9% of the chord	0.0% at 0.0% of the chord	0.7112%	0.0%
HN-276SA	8.85% at 28.7% of the chord	0.35% at 46.9% of the chord	0.6743%	0.0%
HN-304	10.85% at 31.6% of the chord	2.38% at 46.9% of the chord	0.8014%	0.0%
HN-304TA	11.05% at 31.6% of the chord	2.41% at 46.9% of the chord	0.8285%	0.0%
HN-309	10.85% at 31.6% of the chord	2.08% at 46.9% of the chord	0.8021%	0.0%
HN-311S	7.65% at 28.7% of the chord	0.0% at 62.4% of the chord	0.5144%	0.0%
HN-312S	9.55% at 28.7% of the chord	0.0% at 65.5% of the chord	0.756%	0.0%
HN-315S	7.99% at 25.3% of the chord	0.0% at 0.0% of the chord	0.6083%	0.0%
HN-316S	8.85% at 25.3% of the chord	0.0% at 0.0% of the chord	0.7171%	0.0%
HN-319	11.48% at 31.6% of the chord	2.38% at 46.9% of the chord	0.8918%	0.0%
HN-321	7.85% at 31.6% of the chord	1.55% at 43.7% of the chord	0.4912%	0.0%
HN-326	7.84% at 25.9% of the chord	1.65% at 43.7% of the chord	0.5586%	0.0%
HN327	7.84% at 25.9% of the chord	1.85% at 43.7% of the chord	0.5516%	0.0%
HN-333	8.44% at 31.6% of the chord	2.01% at 46.9% of the chord	0.5146%	0.0%
HN-350	7.84% at 31.6% of the chord	1.94% at 43.7% of the chord	0.4605%	0.0%
HN-350M01	8.99% at 31.6% of the chord	1.94% at 43.7% of the chord	0.5739%	0.0%
HN-350M02	8.84% at 31.6% of the chord	2.33% at 43.7% of the chord	0.5562%	0.0%
HN-352	7.98% at 31.6% of the chord	1.54% at 43.7% of the chord	0.4829%	0.0%
HN-354	7.88% at 31.6% of the chord	1.93% at 43.7% of the chord	0.4716%	0.0%
HN-354A	8.5% at 31.6% of the chord	2.0% at 43.7% of the chord	0.5381%	0.0%
HN-354E	8.05% at 31.6% of the chord	1.93% at 43.7% of the chord	0.4911%	0.0%
HN-354ES	8.05% at 31.6% of the chord	1.55% at 43.7% of the chord	0.4969%	0.0%
HN-354OC	8.55% at 31.6% of the chord	2.65% at 43.7% of the chord	0.5392%	0.0%
HN-354SM	8.38% at 31.6% of the chord	2.34% at 43.7% of the chord	0.5174%	0.0%
HN-354SR	8.05% at 31.6% of the chord	1.64% at 43.7% of the chord	0.4805%	0.0%
HN-360	8.33% at 31.6% of the chord	2.15% at 46.9% of the chord	0.5031%	0.0%
HN-409	10.48% at 31.6% of the chord	2.55% at 46.9% of the chord	0.7466%	0.0%
HN-411	11.14% at 31.6% of the chord	2.38% at 46.9% of the chord	0.7799%	0.0%
HN-417	8.04% at 25.9% of the chord	2.28% at 43.7% of the chord	0.5662%	0.0%
HN-418	8.55% at 28.7% of the chord	2.48% at 43.7% of the chord	0.5975%	0.0%
HN-419	7.77% at 25.9% of the chord	2.38% at 43.7% of the chord	0.5432%	0.0%
HN-424	8.85% at 28.7% of the chord	2.63% at 43.7% of the chord	0.6335%	0.0%
HN-436	8.5% at 28.7% of the chord	1.65% at 46.9% of the chord	0.581%	0.0%
HN-446	7.84% at 28.7% of the chord	1.71% at 46.9% of the chord	0.5164%	0.0%
HN-450	8.32% at 31.6% of the chord	1.88% at 40.6% of the chord	0.497%	0.0%
HN-450S	8.54% at 31.6% of the chord	1.85% at 40.6% of the chord	0.5181%	0.0%
HN-462	8.08% at 31.6% of the chord	1.34% at 43.7% of the chord	0.4933%	0.0%

Note:

Hatschek (J. Hatschek (Czechoslovakia));
HD45, HD46, HD47, HD48, HD48A, HD48B, HD50, HD53, HD54, HD800, HD801 (Hannes Delago);
Hill SR 2 (M. Hill (USA));
HL 73-6508, HL 74-3512, HL 74-5508, HL 75-5414, HL 75-K-3308, HL 80-13353 (B. Horeni – J. Lnenka (Czechoslovakia));
HN 380 (F3B – RCM 205 de 1998);
HN-003, HN-1023, HN-188, HN-203, HN-304, HN-304TA, HN-309, HN-319, HN-409, HN-411 (Planeur>3.5m, Norbert Habbe);
HN-032, HN-036, HN-038, HN-1038, HN-321, HN-326, HN-354ES, HN-354SR, HN-436, HN-446, HN-462 (F3F Norbert Habbe);
HN-033, HN-163, HN-163TA, HN-163TB, HN-184, HN-216, HN-216TA, HN327, HN-350, HN-354, HN-354E (F3B Norbert Habbe);
HN-034, HN-035 (F3 Norbert Habbe);
HN-1027, HN-1029, HN-1033, HN-1033A, HN-1070, HN-419 (HLG Norbert Habbe);
HN-1036, HN-1051, HN-1054, HN-184M, HN-418, HN-424, HN-450, HN-450S (Planeur Norbert Habbe);
HN-153S, HN-274S, HN-275S, HN-276SA, HN-311S, HN-312S, HN-315S, HN-316S (Aile volante Norbert Habbe);
HN-211 (F3F-F3B Norbert Habbe);
HN-217, HN-227, HN-239, HN-333, HN-350M01, HN-350M02, HN-352, HN-354OC, HN-354SM, HN-360, HN-417 (F3J Norbert Habbe);
HN-354A (BASIC Norbert Habbe).

Table 2. The geometric shapes of the airfoils in the cross section.

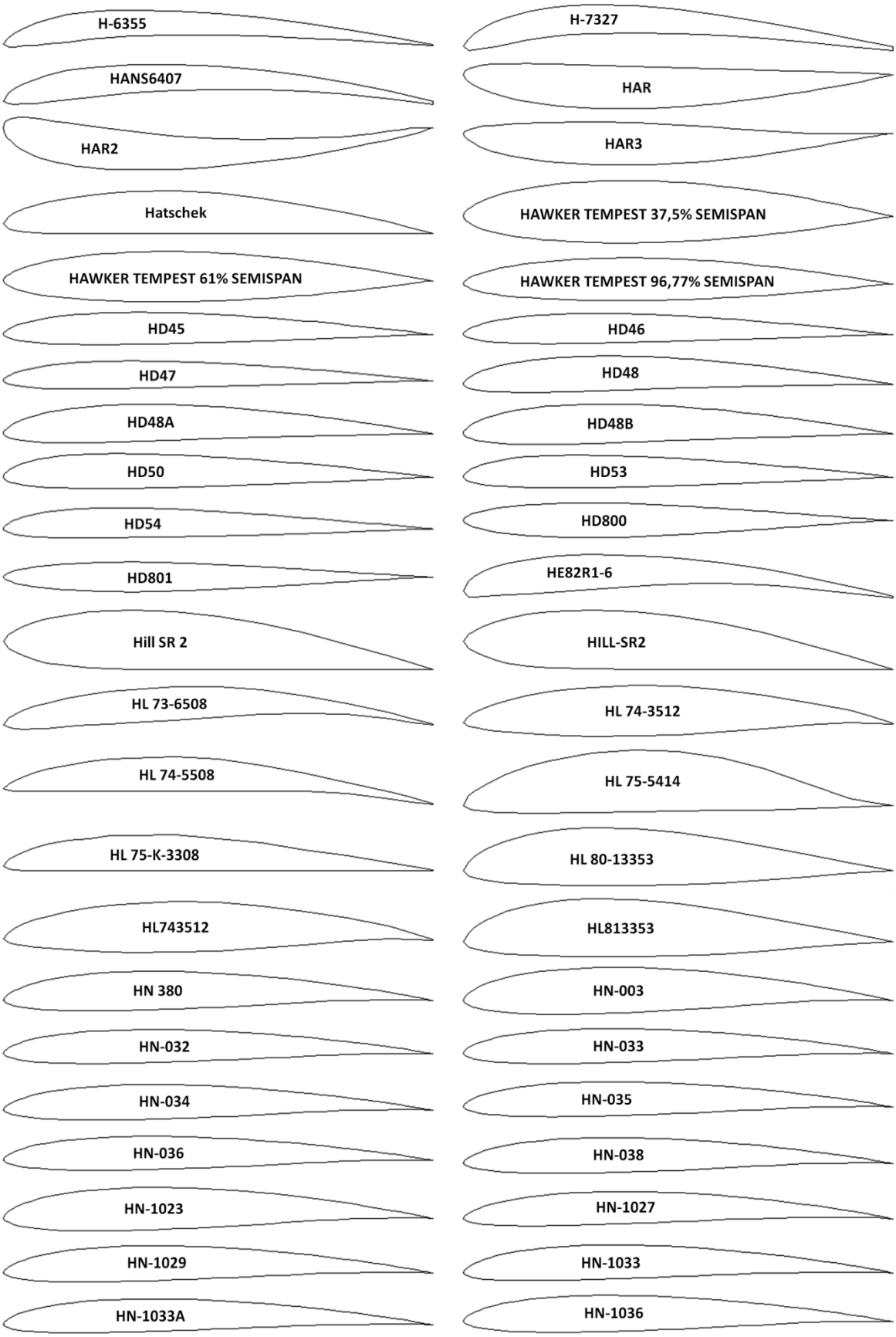

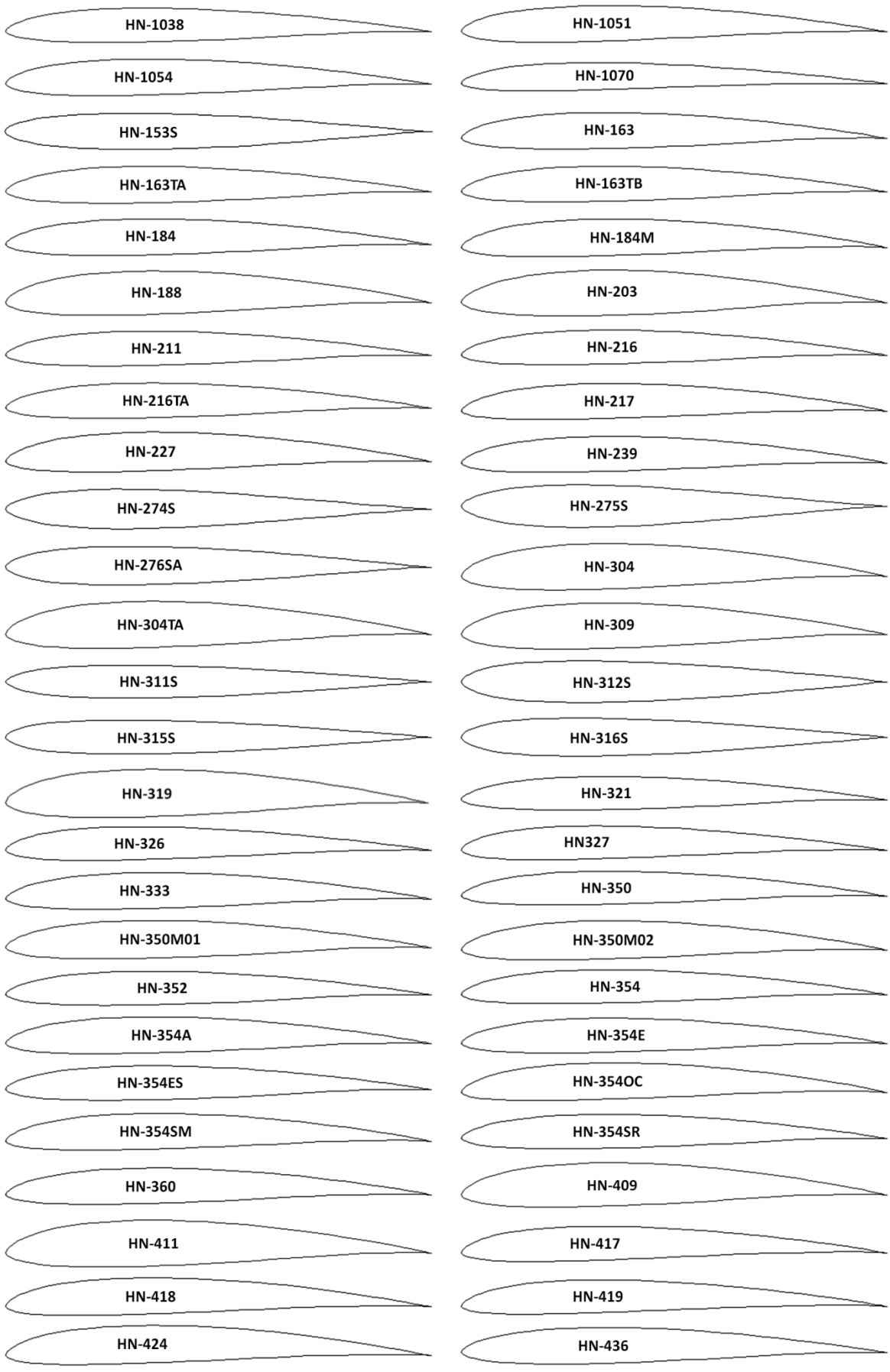
HN-1038
HN-1051
HN-1054
HN-1070
HN-153S
HN-163
HN-163TA
HN-163TB
HN-184
HN-184M
HN-188
HN-203
HN-211
HN-216
HN-216TA
HN-217
HN-227
HN-239
HN-274S
HN-275S
HN-276SA
HN-304
HN-304TA
HN-309
HN-311S
HN-312S
HN-315S
HN-316S
HN-319
HN-321
HN-326
HN327
HN-333
HN-350
HN-350M01
HN-350M02
HN-352
HN-354
HN-354A
HN-354E
HN-354ES
HN-354OC
HN-354SM
HN-354SR
HN-360
HN-409
HN-411
HN-417
HN-418
HN-419
HN-424
HN-436

Results and discussion

The calculated pressure contours on the surfaces of the airfoils at the different angles of attack are presented in the Figs. 1-102. The calculated values on the scale can be represented as the basic values when comparing the pressure drop under conditions of changing the angle of attack of the airfoils.

102 airfoils of the HN, HL, HD, HAR, etc. series were studied in this work. The airfoils are represented by asymmetrical geometries and symmetrical geometries (HN-153S, HN-274S, HN-275S, HN-311S, HN-312S, HN-315S and HN-316S) in the cross section.

The greatest drag value was determined on the leading edge of the Hill SR 2 airfoil. The drag coefficient was calculated from the calculated value of positive pressure (6.63 kPa) that occurs on the leading edge of the airplane wing flying horizontally. Similarly, the lowest drag value (3.75 kPa) was obtained on the leading edges of the HN-1027 and HN-311S airfoils. Thus, the drag value of the airfoils of the HN series is almost 2 times less than that of the airfoils of other series. This decrease in the drag is noted for the HN-038 – HN-462 airfoils. The analysis of the calculation results showed that at the positive angles of attack, maximum negative pressure is formed on the surfaces of the airfoils. In particular, the negative pressure value is -82 kPa for the HN-035 airfoil. The action of positive and negative pressures of the small value (from 4 to -15 kPa) on the surfaces and the edges is observed at the negative angles of attack of the most airfoils of the HN series.

Let us consider in detail some airfoils that have the special geometric shapes in the cross section. The HAR2 airfoil, compared to the other two airfoils in this series, is subjected to less negative pressure during the airplane descent. The camber of the airfoil leads to the formation of areas of positive and negative pressures along the entire length of the upper surface. The descent and horizontal flight of the airplane with the HL 74-5508 wing airfoil are characterized by a minimum difference (about 1.0 kPa) of positive and negative pressures arising on the surfaces and the edges. The asymmetrical shape of the Hill SR 2 airfoil ensures the formation of the pressures areas of almost the same value during the airplane maneuvers.

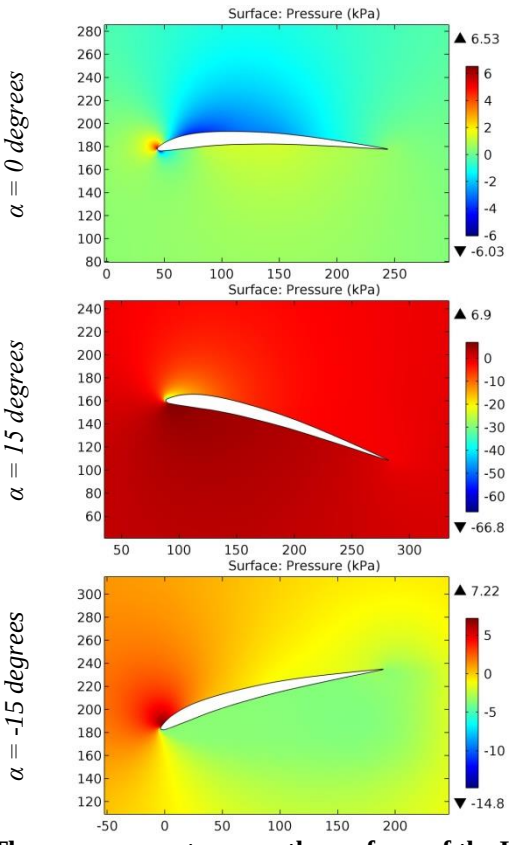

Figure 1. The pressure contours on the surfaces of the H-6355 airfoil.

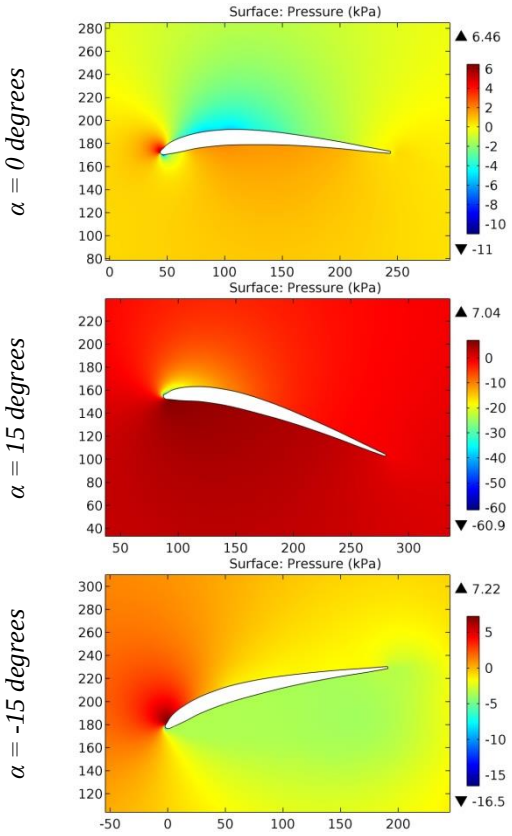

Figure 2. The pressure contours on the surfaces of the H-7327 airfoil.

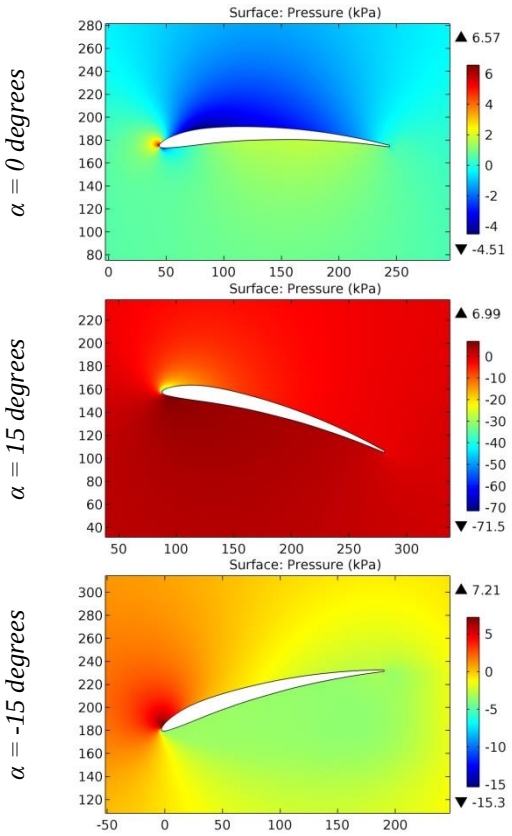

Figure 3. The pressure contours on the surfaces of the HANS6407 airfoil.

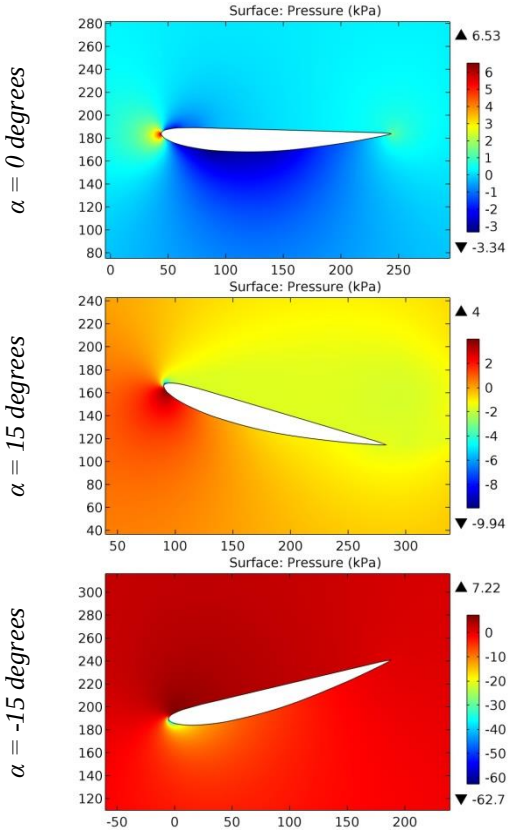

Figure 4. The pressure contours on the surfaces of the HAR airfoil.

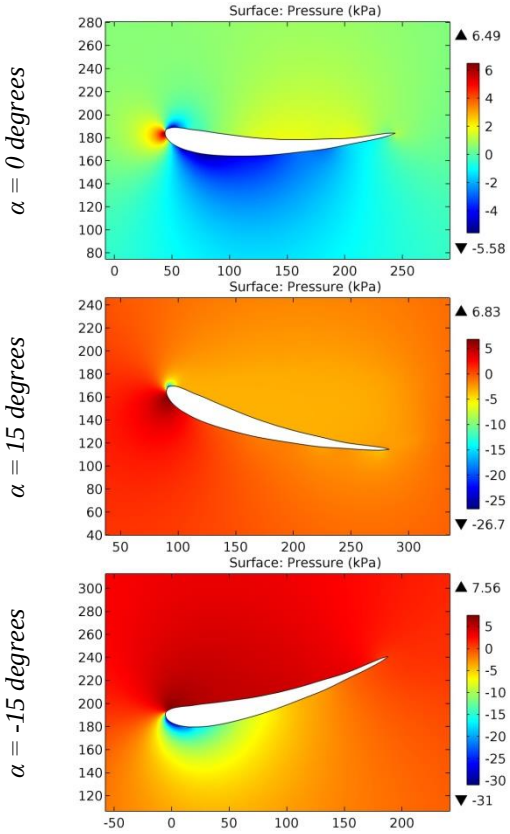

Figure 5. The pressure contours on the surfaces of the HAR2 airfoil.

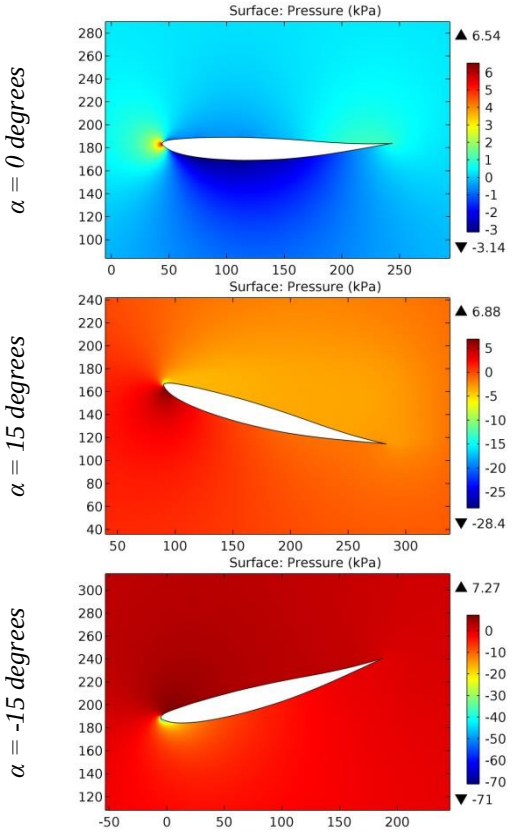

Figure 6. The pressure contours on the surfaces of the HAR3 airfoil.

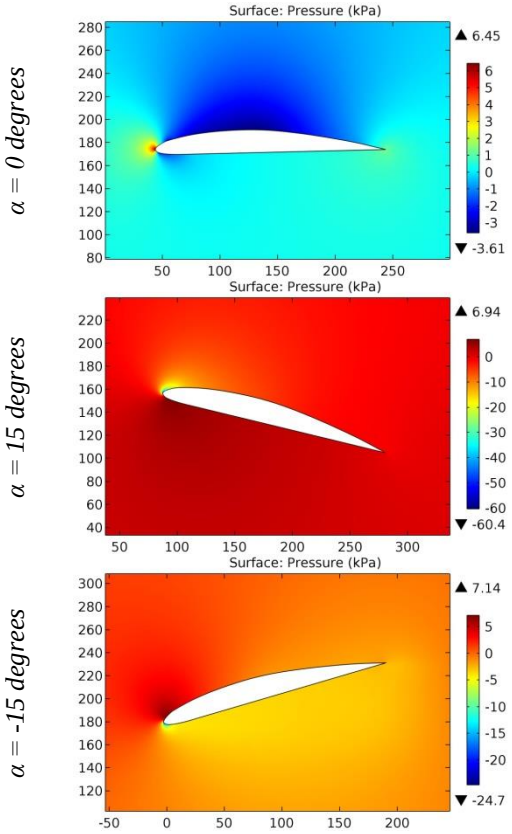

Figure 7. The pressure contours on the surfaces of the Hatschek airfoil.

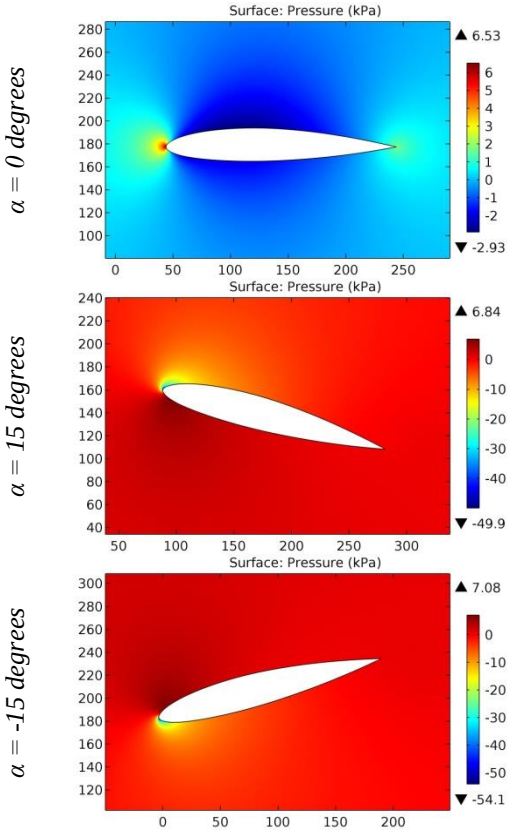

Figure 8. The pressure contours on the surfaces of the HAWKER TEMPEST 37,5% SEMISPAN airfoil.

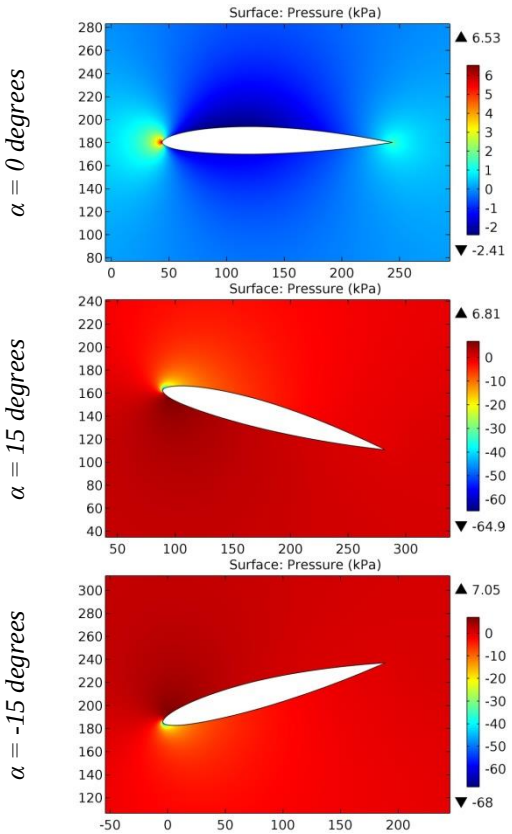

Figure 9. The pressure contours on the surfaces of the HAWKER TEMPEST 61% SEMISPAN airfoil.

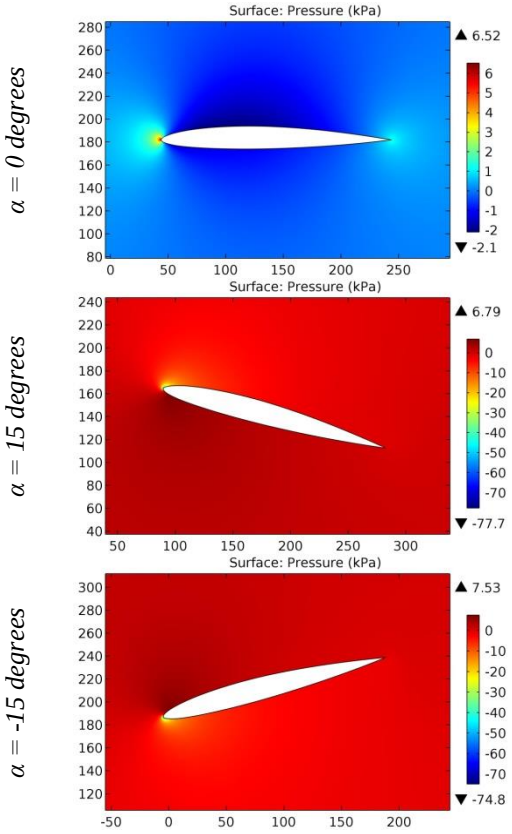

Figure 10. The pressure contours on the surfaces of the HAWKER TEMPEST 96,77% SEMISPAN airfoil.

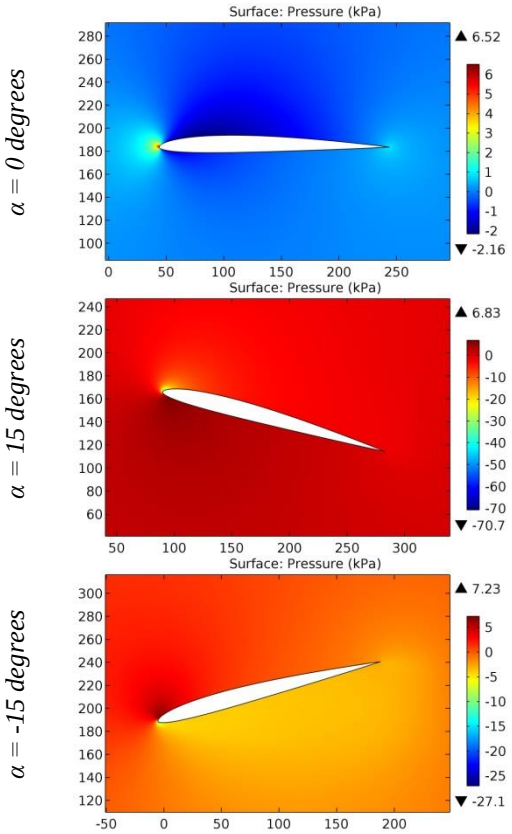

Figure 11. The pressure contours on the surfaces of the HD45 airfoil.

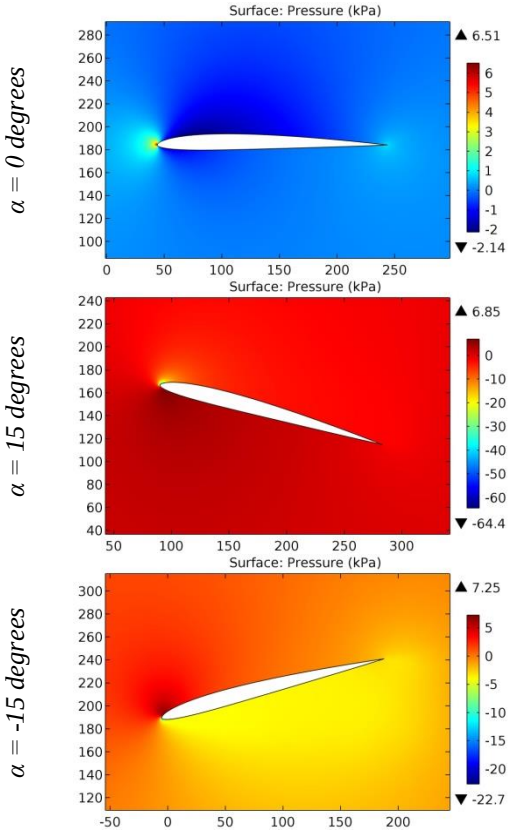

Figure 12. The pressure contours on the surfaces of the HD46 airfoil.

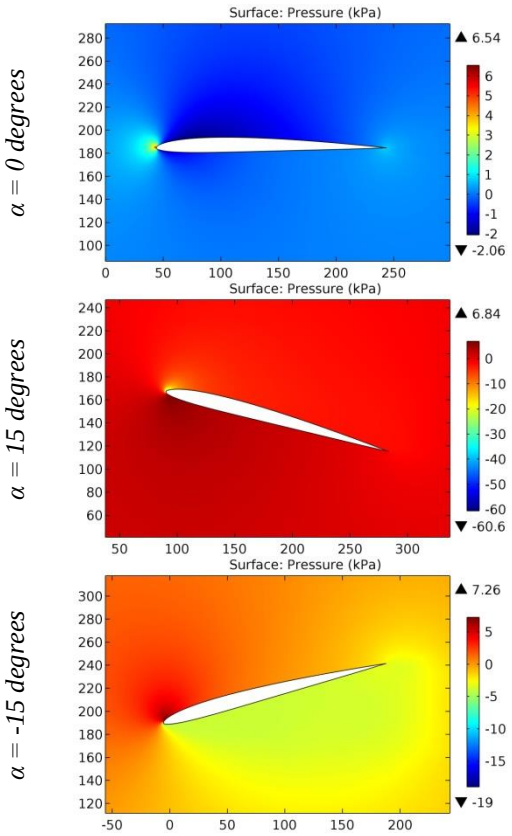

Figure 13. The pressure contours on the surfaces of the HD47 airfoil.

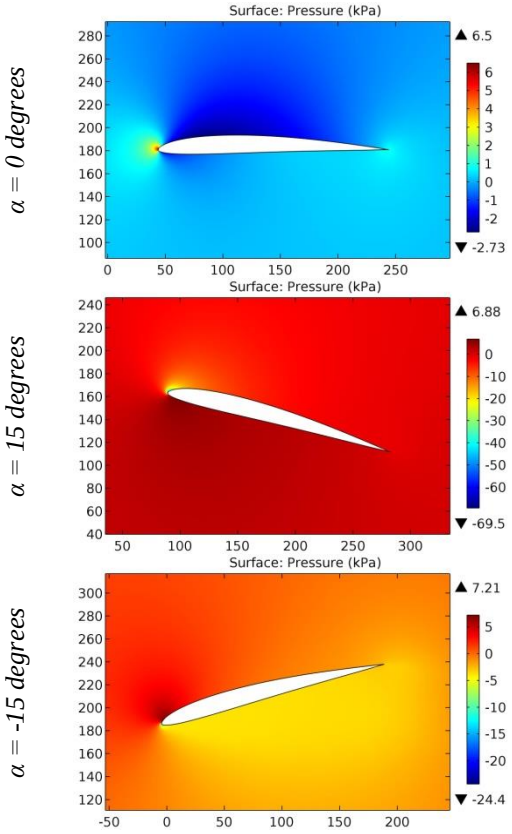

Figure 14. The pressure contours on the surfaces of the HD48 airfoil.

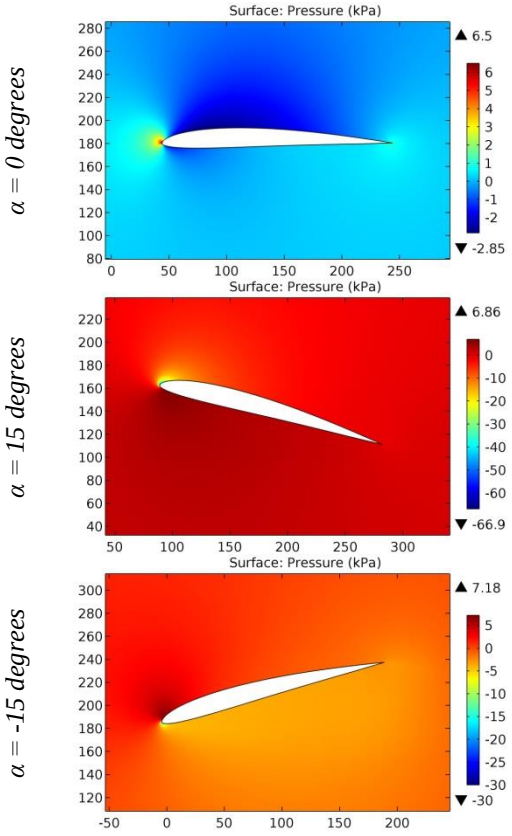

Figure 15. The pressure contours on the surfaces of the HD48A airfoil.

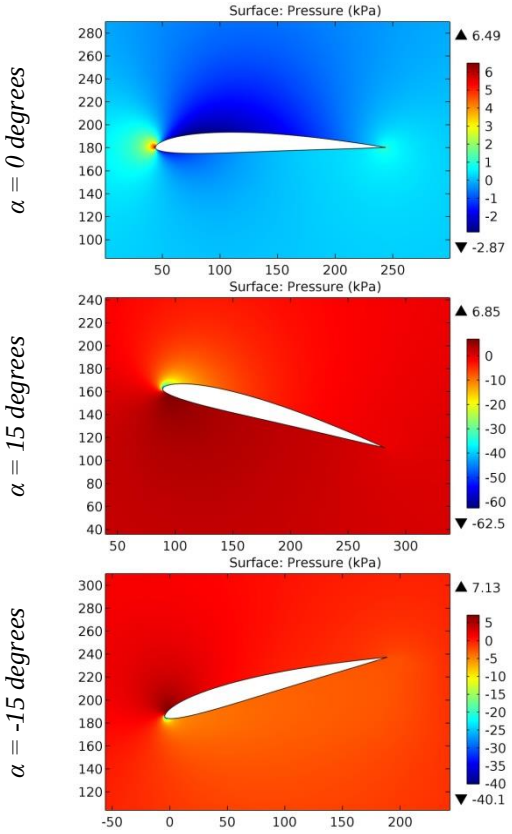

Figure 16. The pressure contours on the surfaces of the HD48B airfoil.

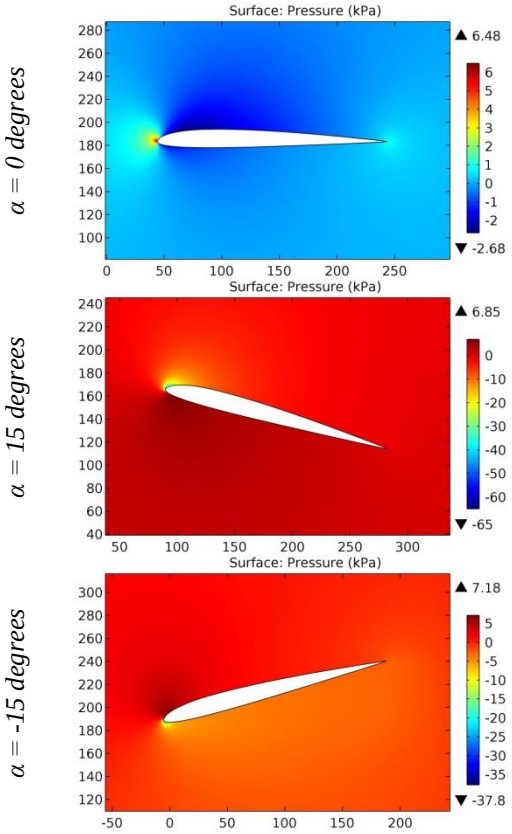

Figure 17. The pressure contours on the surfaces of the HD50 airfoil.

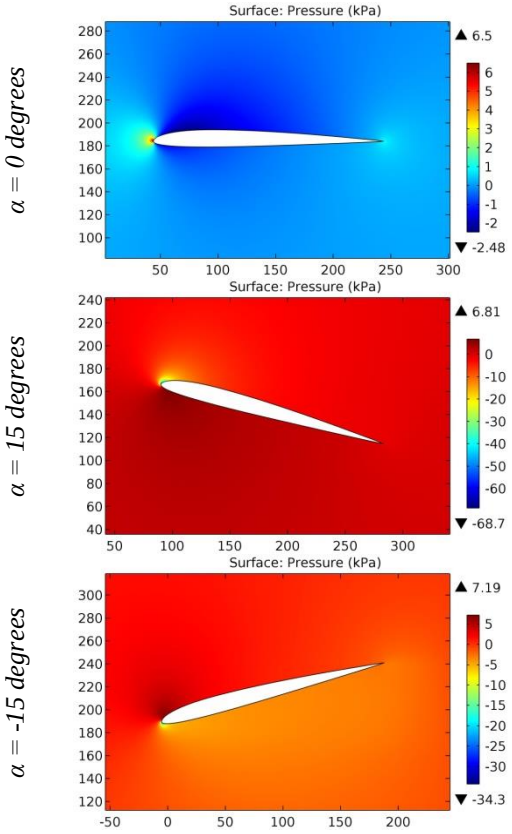

Figure 18. The pressure contours on the surfaces of the HD53 airfoil.

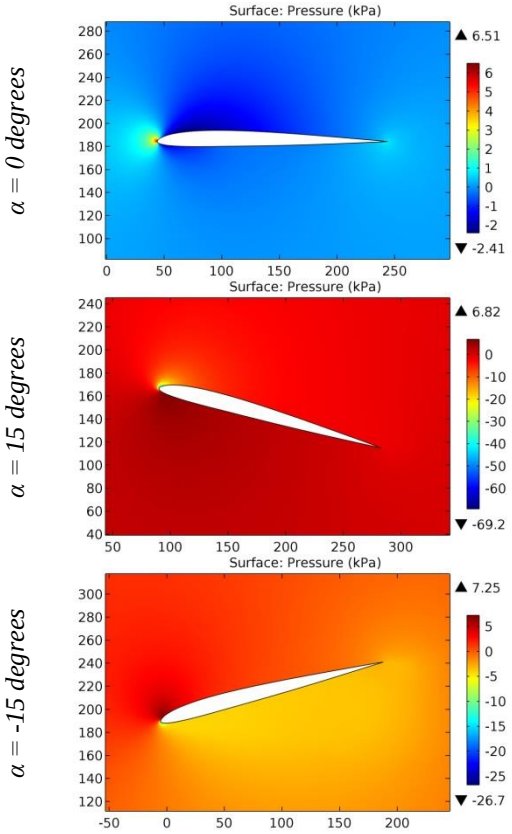

Figure 19. The pressure contours on the surfaces of the HD54 airfoil.

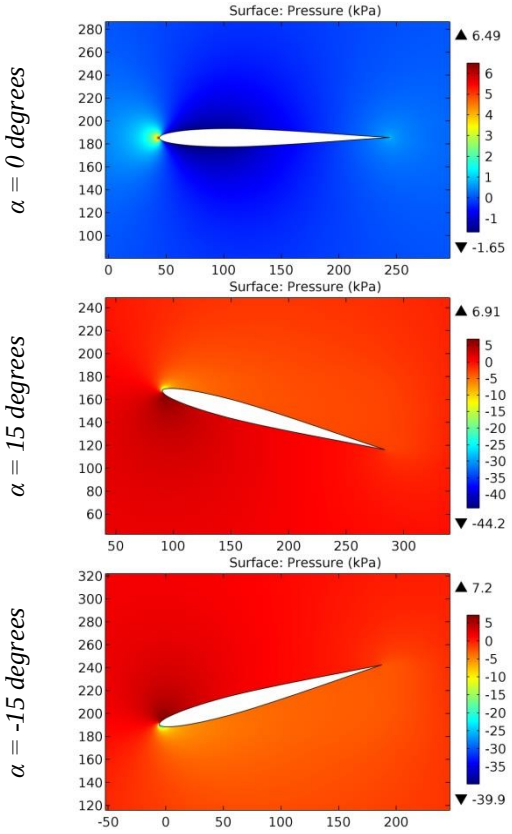

Figure 20. The pressure contours on the surfaces of the HD800 airfoil.

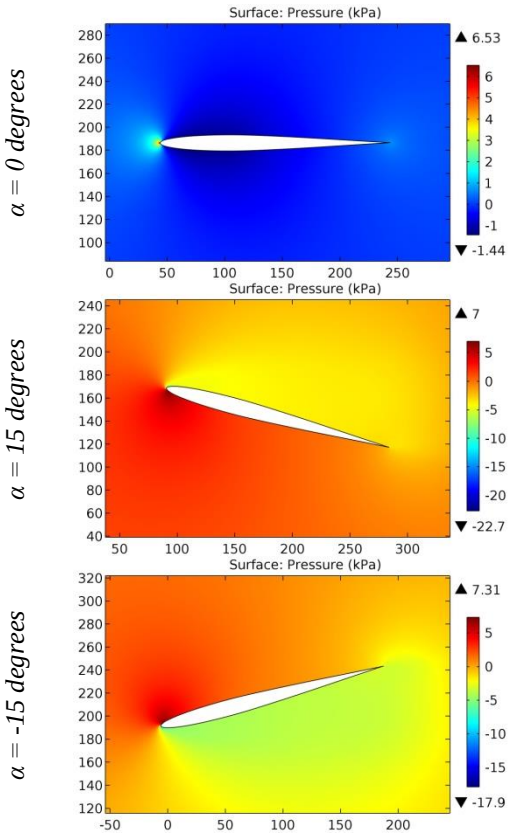

Figure 21. The pressure contours on the surfaces of the HD801 airfoil.

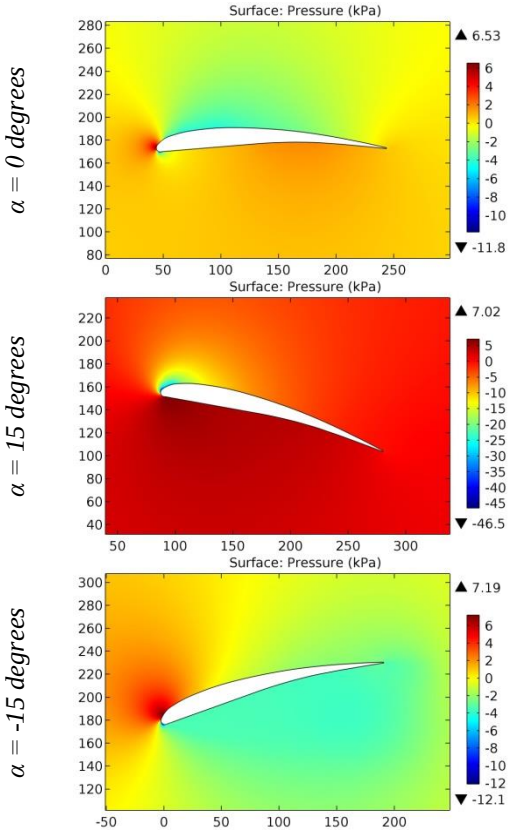

Figure 22. The pressure contours on the surfaces of the HE82R1-6 airfoil.

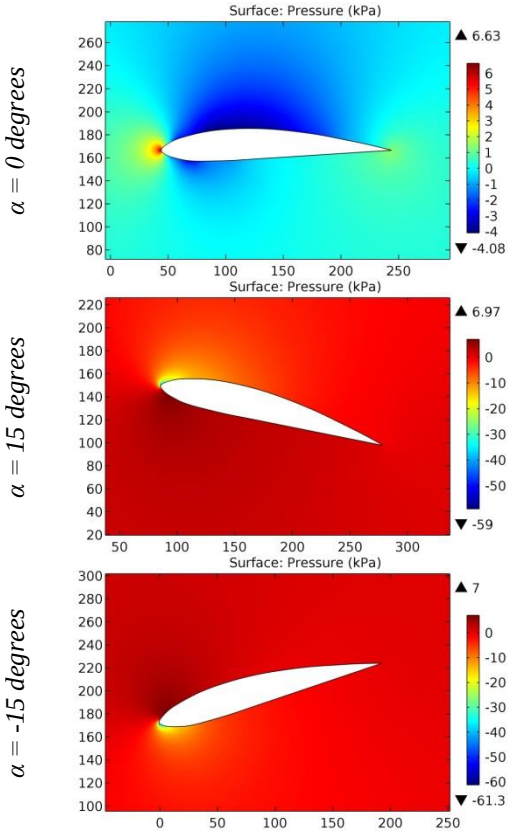

Figure 23. The pressure contours on the surfaces of the Hill SR 2 airfoil.

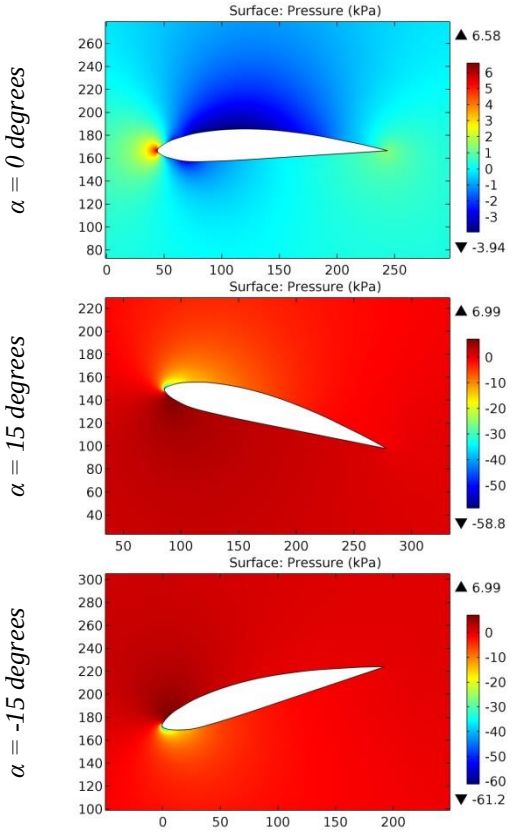

Figure 24. The pressure contours on the surfaces of the HILL-SR2 airfoil.

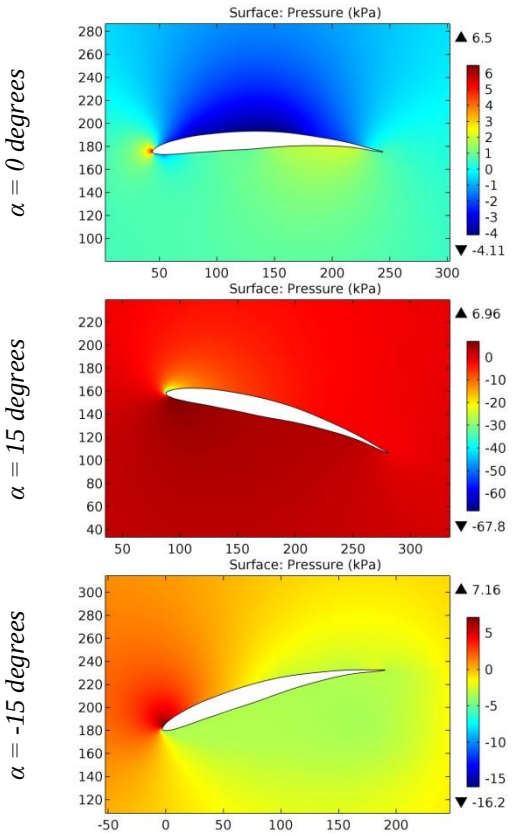

Figure 25. The pressure contours on the surfaces of the HL 73-6508 airfoil.

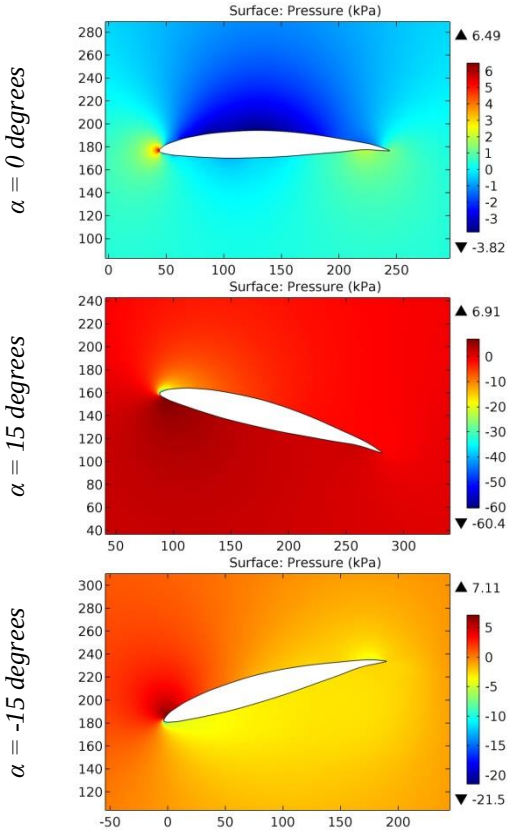

Figure 26. The pressure contours on the surfaces of the HL 74-3512 airfoil.

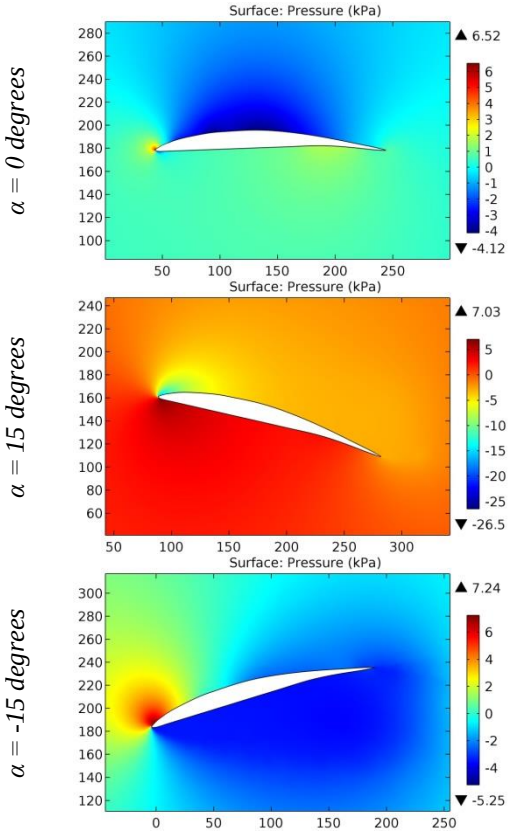

Figure 27. The pressure contours on the surfaces of the HL 74-5508 airfoil.

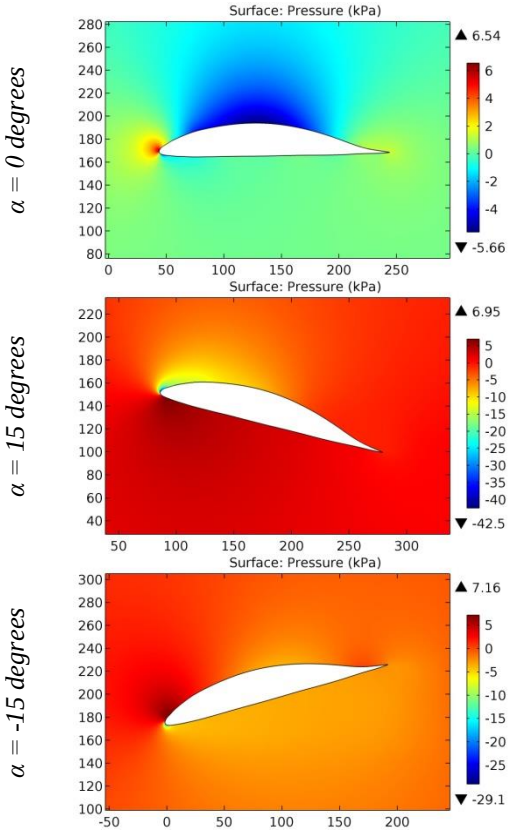

Figure 28. The pressure contours on the surfaces of the HL 75-5414 airfoil.

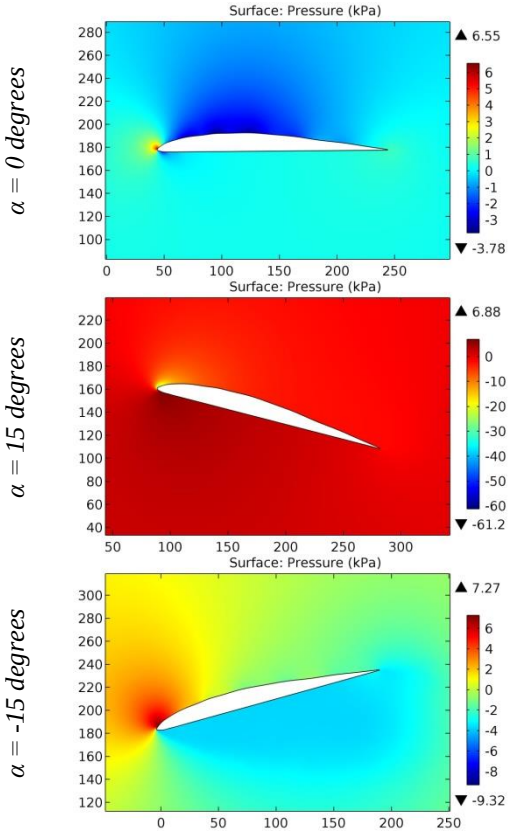

Figure 29. The pressure contours on the surfaces of the HL 75-K-3308 airfoil.

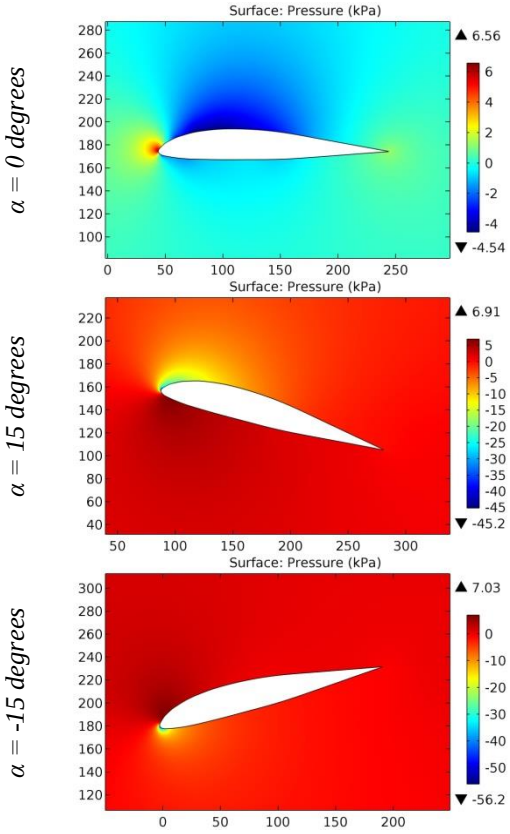

Figure 30. The pressure contours on the surfaces of the HL 80-13353 airfoil.

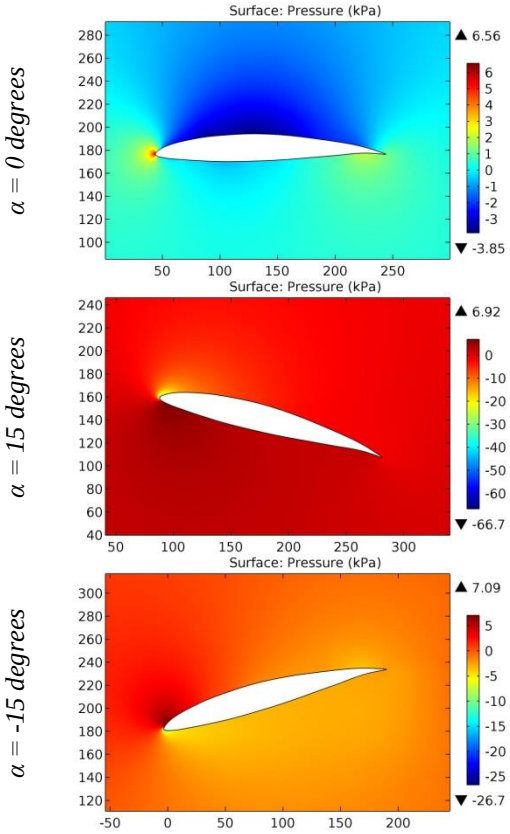

Figure 31. The pressure contours on the surfaces of the HL743512 airfoil.

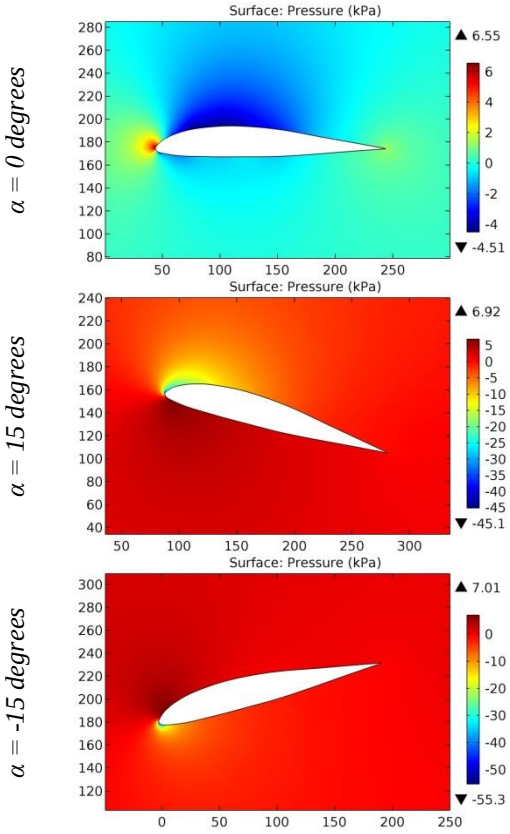

Figure 32. The pressure contours on the surfaces of the HL813353 airfoil.

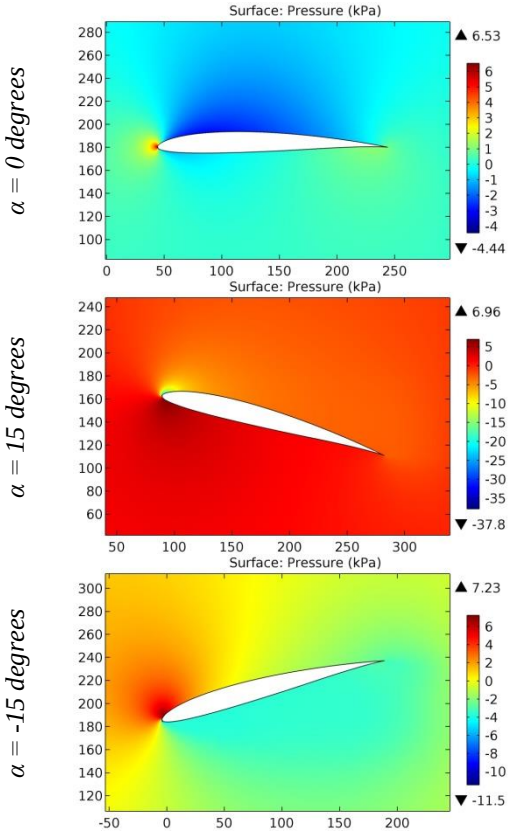

Figure 33. The pressure contours on the surfaces of the HN 380 airfoil.

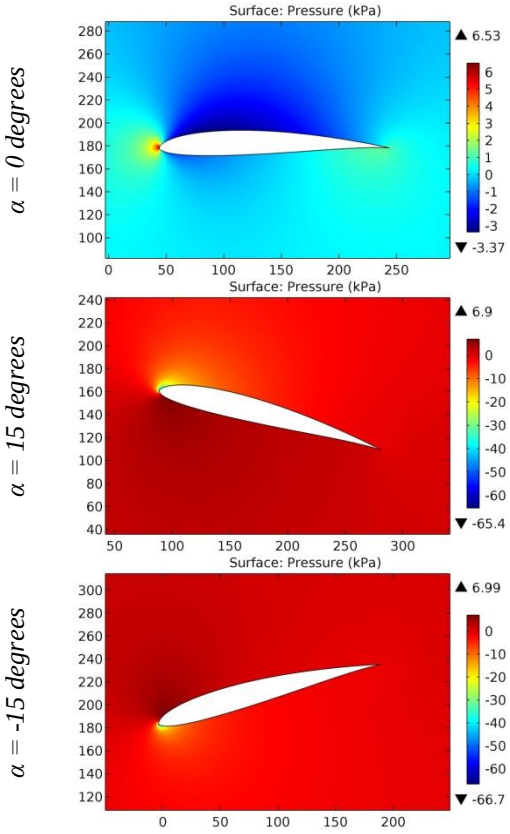

Figure 34. The pressure contours on the surfaces of the HN-003 airfoil.

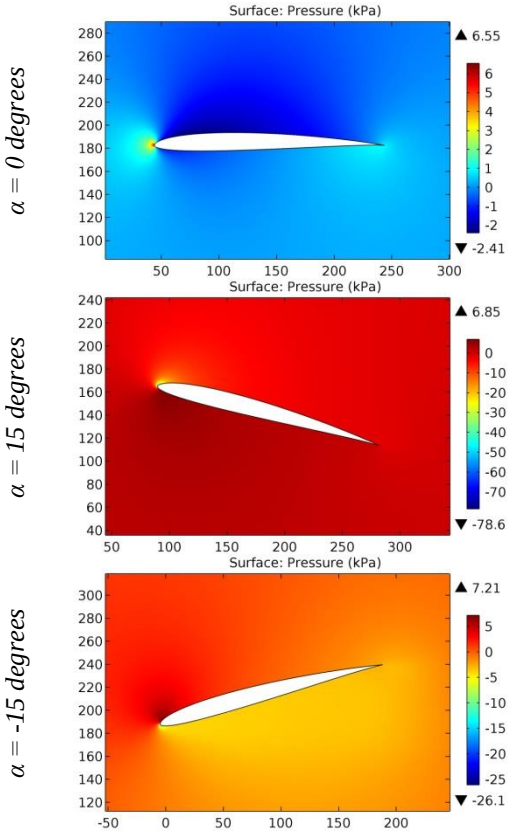

Figure 35. The pressure contours on the surfaces of the HN-032 airfoil.

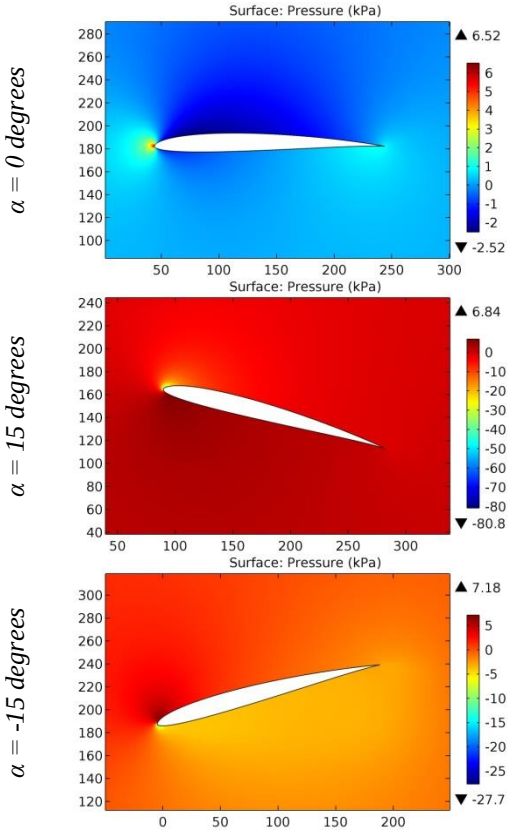

Figure 36. The pressure contours on the surfaces of the HN-033 airfoil.

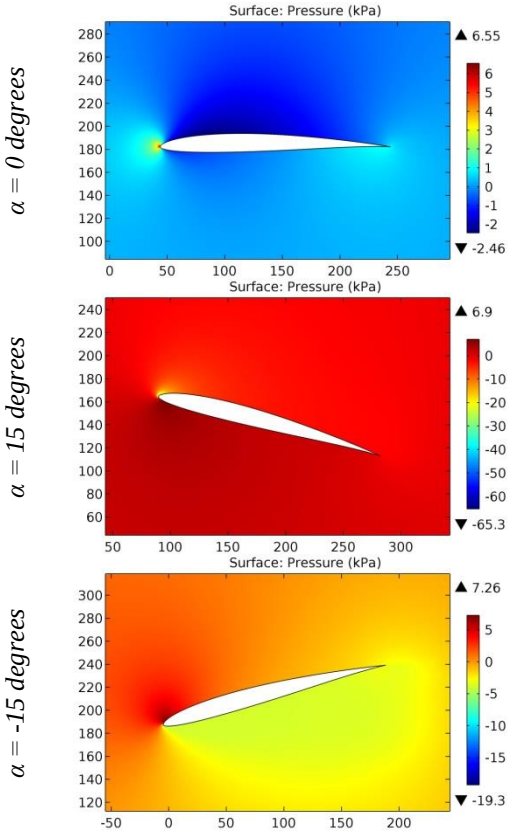

Figure 37. The pressure contours on the surfaces of the HN-034 airfoil.

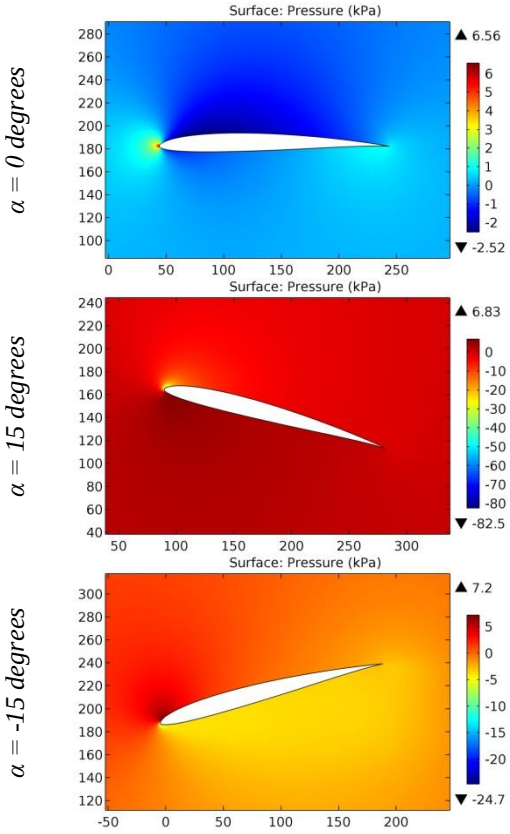

Figure 38. The pressure contours on the surfaces of the HN-035 airfoil.

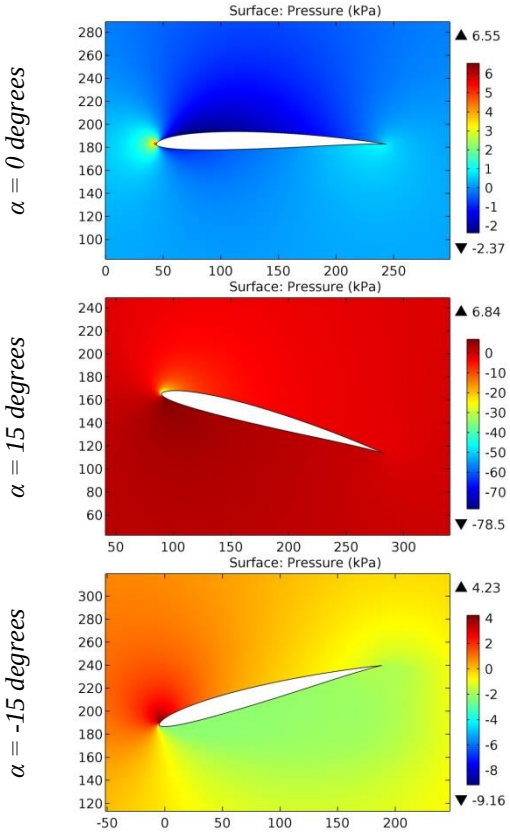

Figure 39. The pressure contours on the surfaces of the HN-036 airfoil.

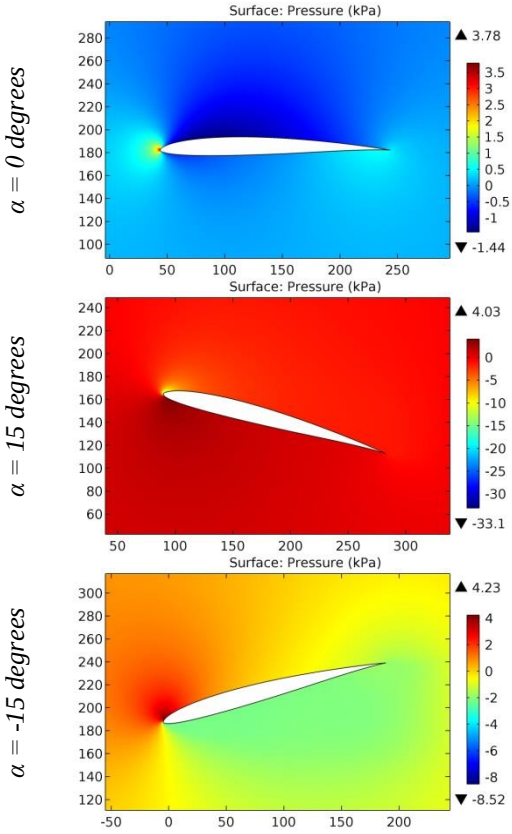

Figure 40. The pressure contours on the surfaces of the HN-038 airfoil.

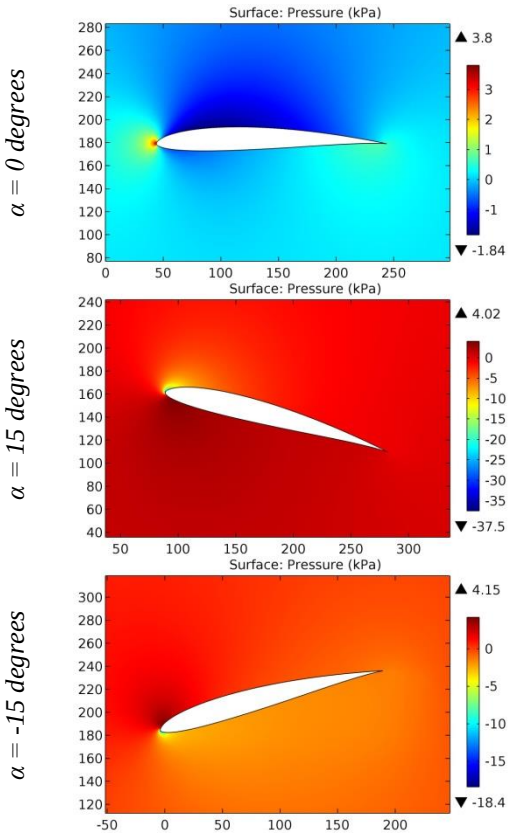

Figure 41. The pressure contours on the surfaces of the HN-1023 airfoil.

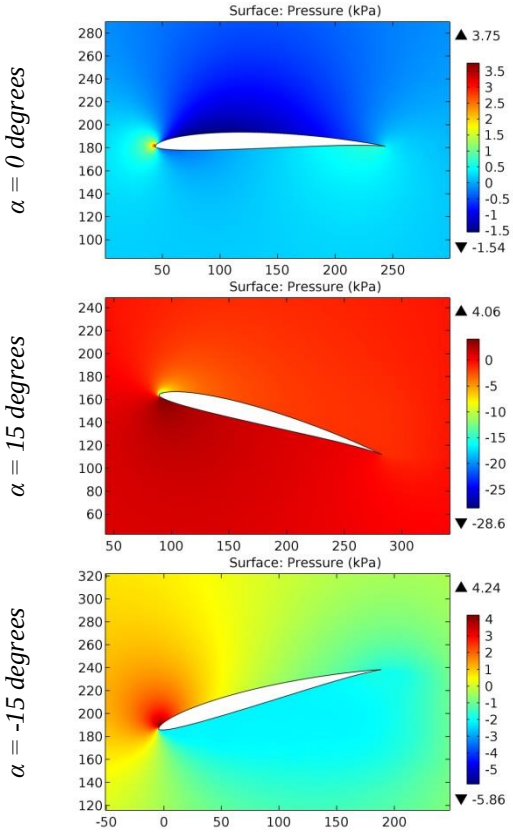

Figure 42. The pressure contours on the surfaces of the HN-1027 airfoil.

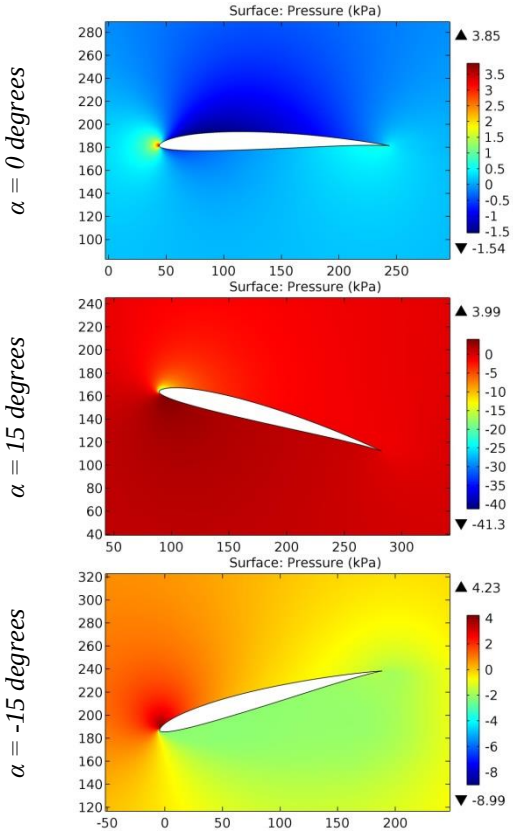

Figure 43. The pressure contours on the surfaces of the HN-1029 airfoil.

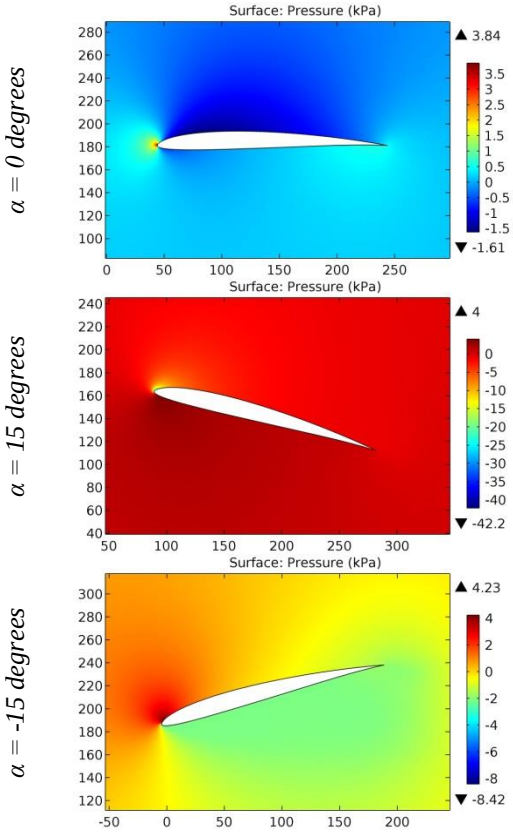

Figure 44. The pressure contours on the surfaces of the HN-1033 airfoil.

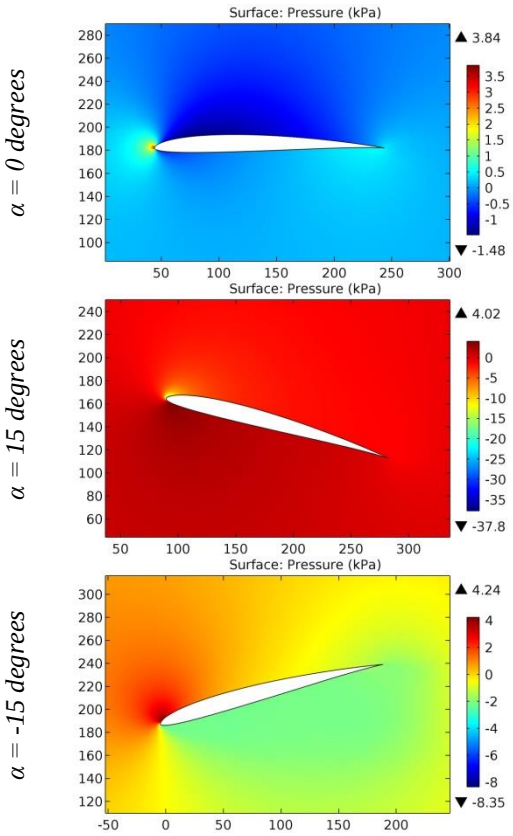

Figure 45. The pressure contours on the surfaces of the HN-1033A airfoil.

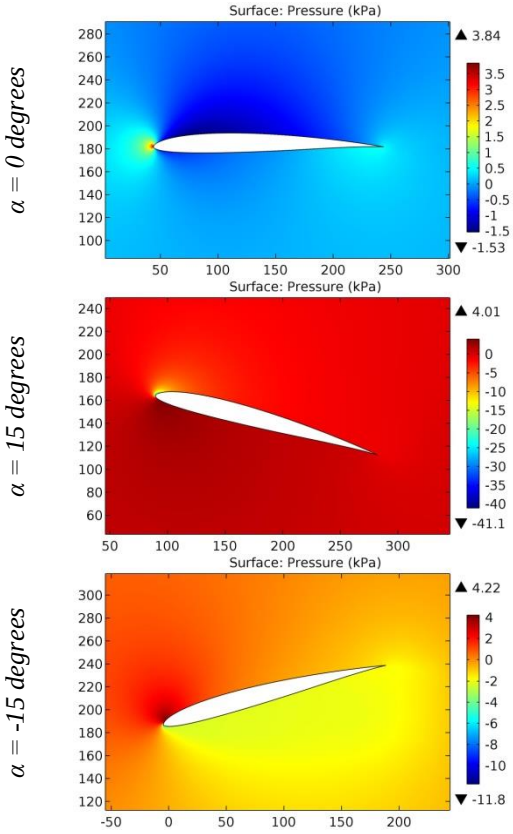

Figure 46. The pressure contours on the surfaces of the HN-1036 airfoil.

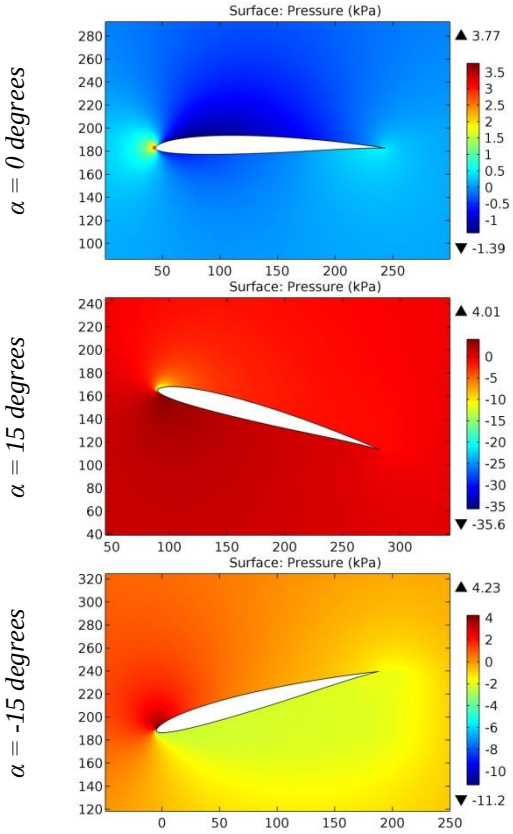

Figure 47. The pressure contours on the surfaces of the HN-1038 airfoil.

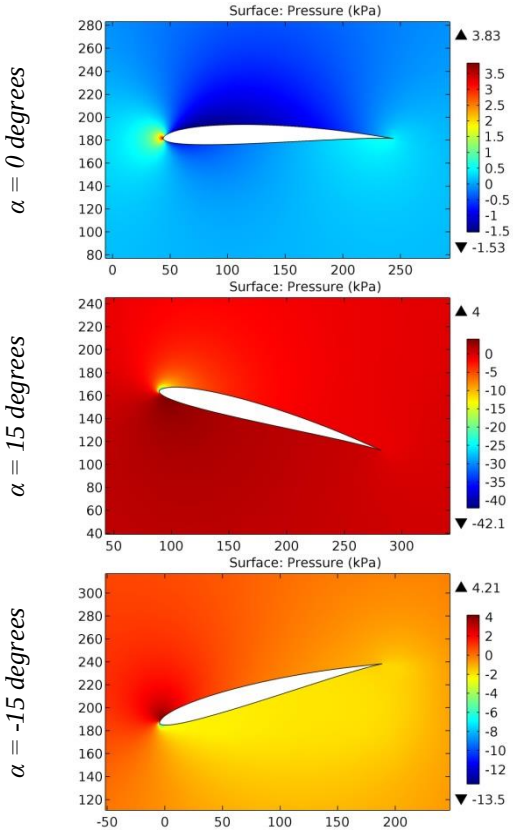

Figure 48. The pressure contours on the surfaces of the HN-1051 airfoil.

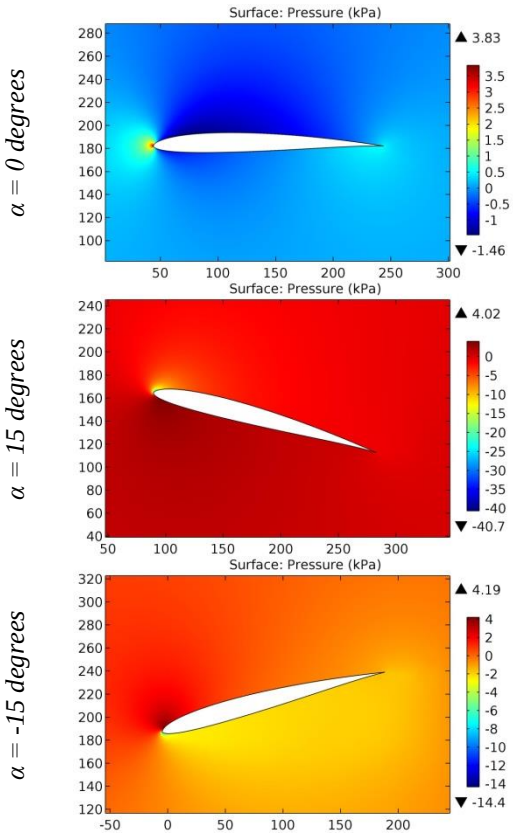

Figure 49. The pressure contours on the surfaces of the HN-1054 airfoil.

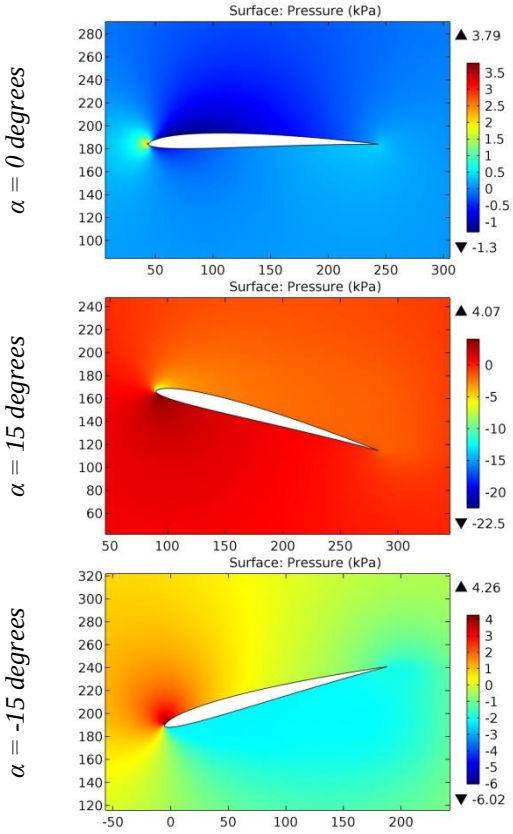

Figure 50. The pressure contours on the surfaces of the HN-1070 airfoil.

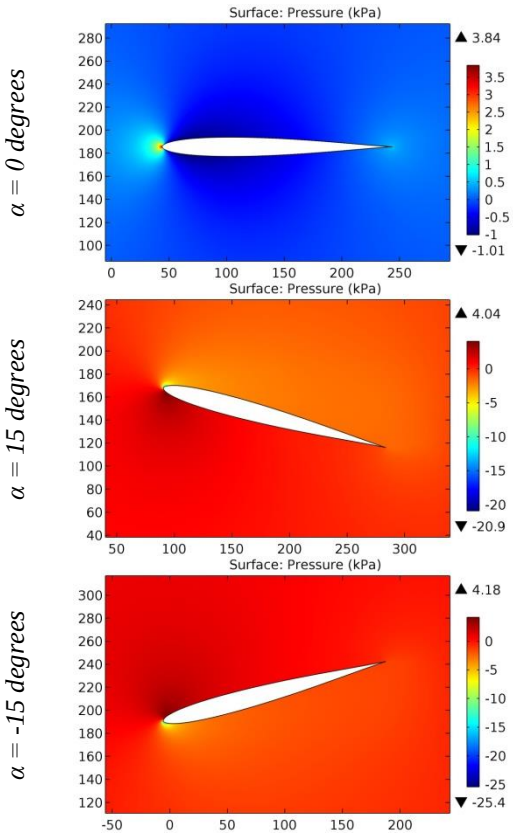

Figure 51. The pressure contours on the surfaces of the HN-153S airfoil.

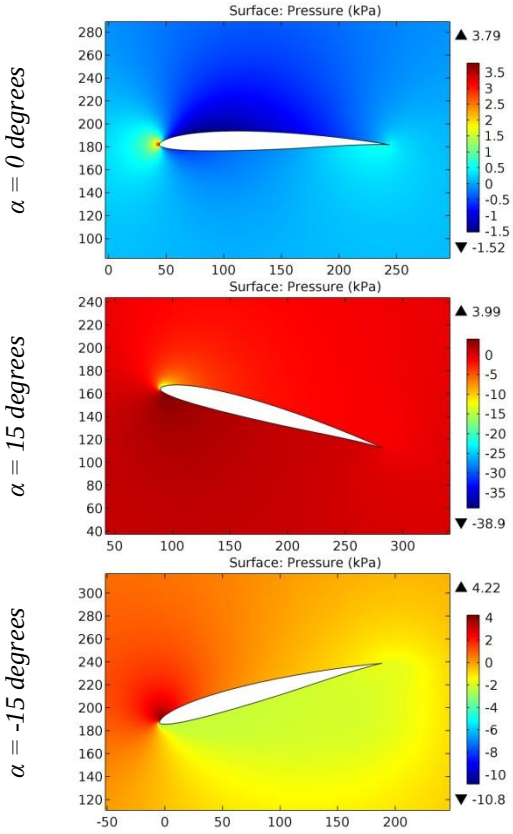

Figure 52. The pressure contours on the surfaces of the HN-163 airfoil.

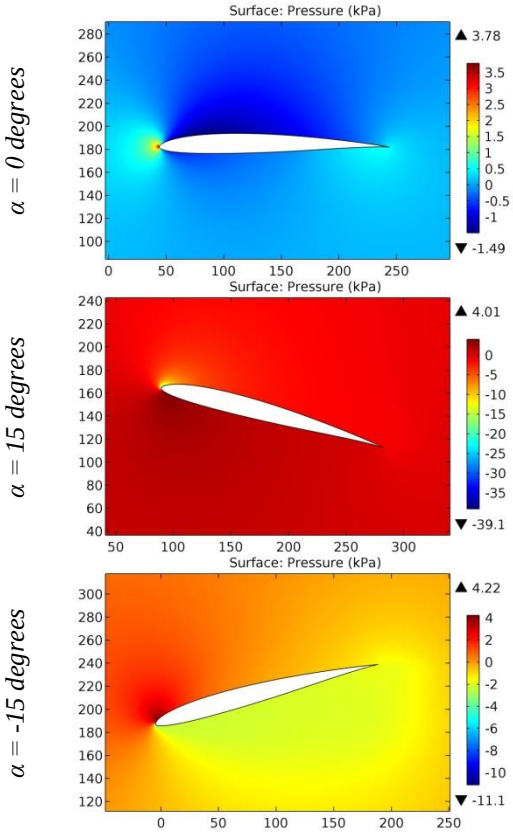

Figure 53. The pressure contours on the surfaces of the HN-163TA airfoil.

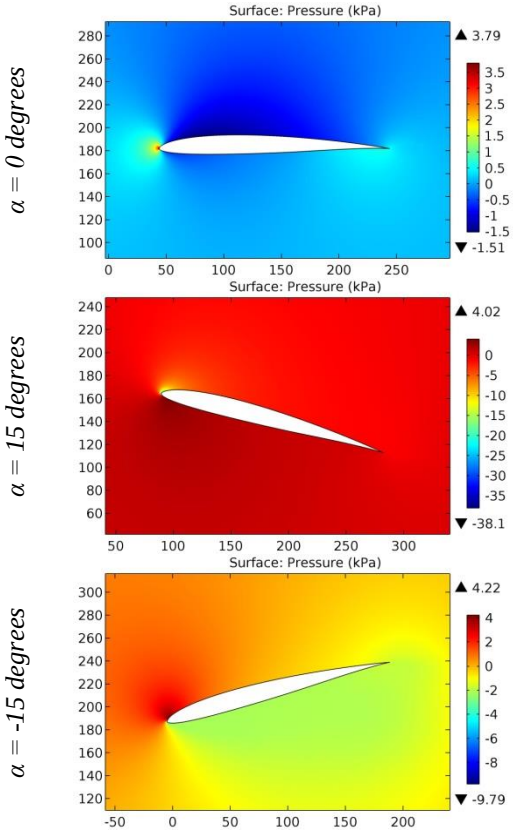

Figure 54. The pressure contours on the surfaces of the HN-163TB airfoil.

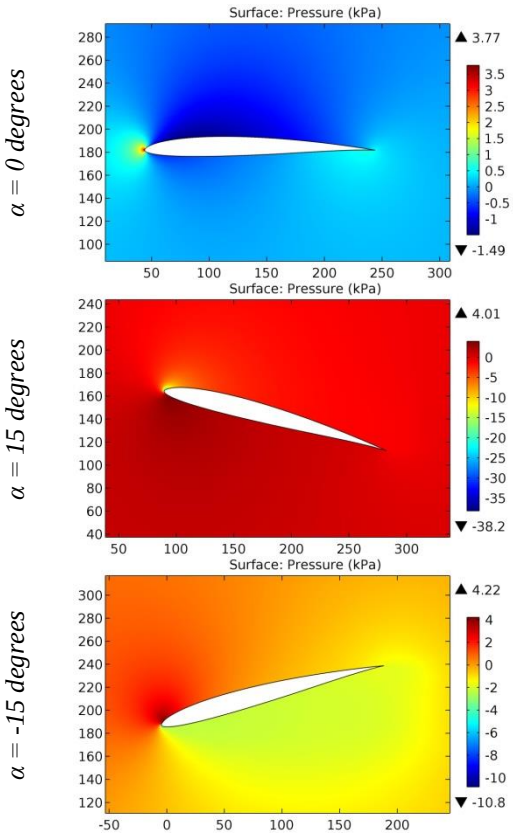

Figure 55. The pressure contours on the surfaces of the HN-184 airfoil.

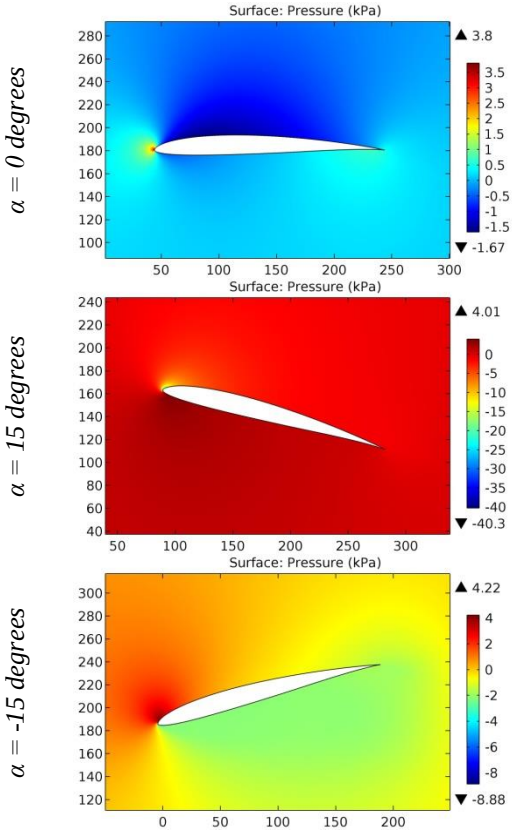

Figure 56. The pressure contours on the surfaces of the HN-184M airfoil.

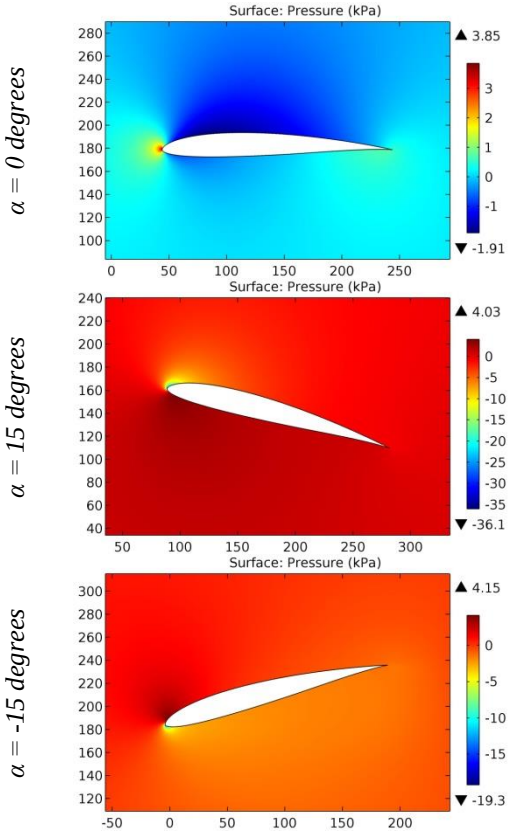

Figure 57. The pressure contours on the surfaces of the HN-188 airfoil.

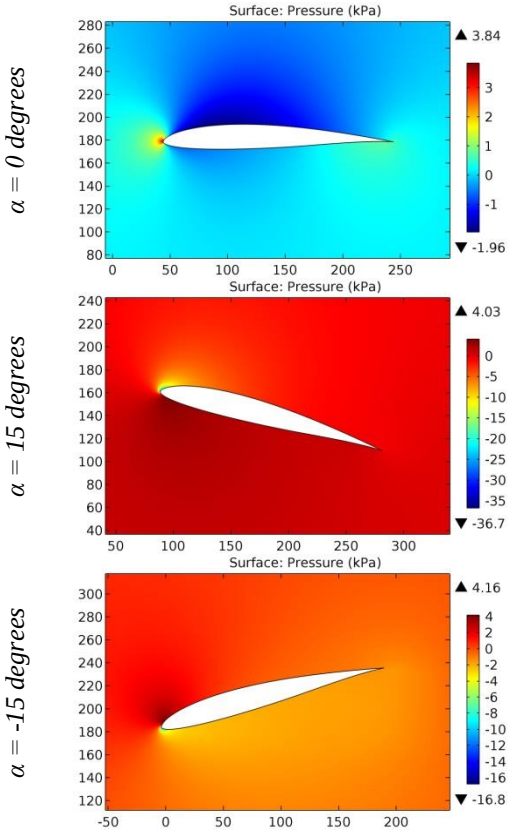

Figure 58. The pressure contours on the surfaces of the HN-203 airfoil.

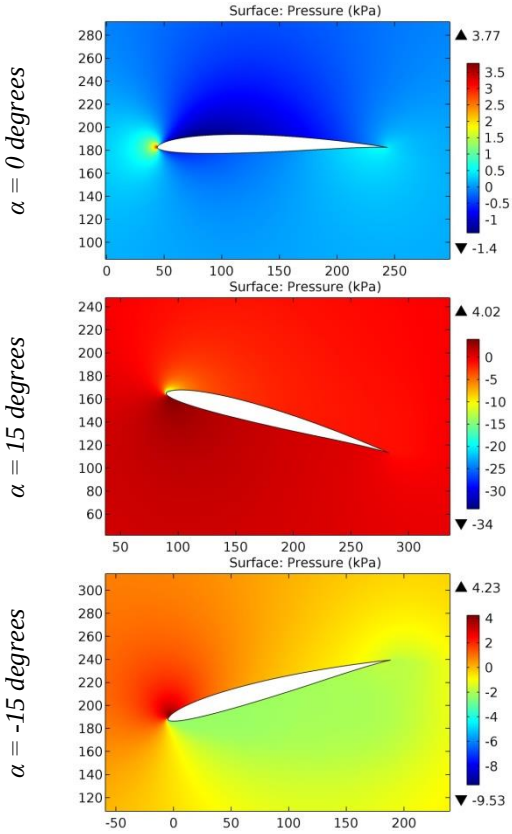

Figure 59. The pressure contours on the surfaces of the HN-211 airfoil.

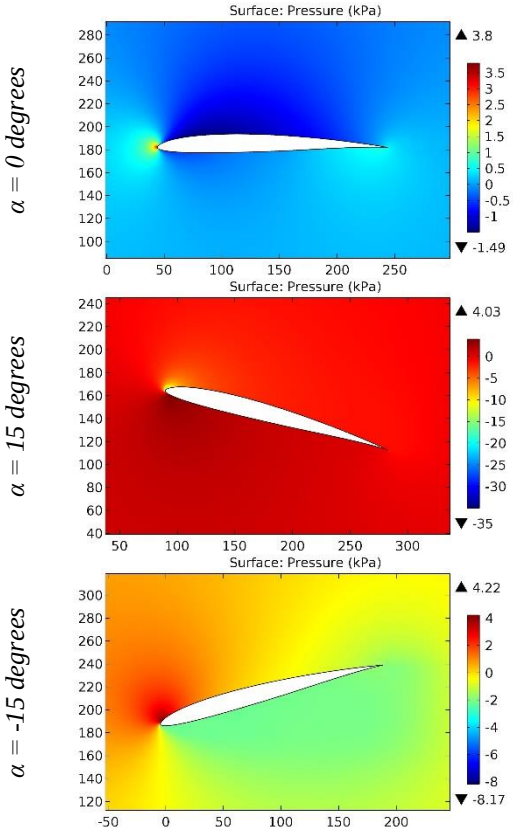

Figure 60. The pressure contours on the surfaces of the HN-216 airfoil.

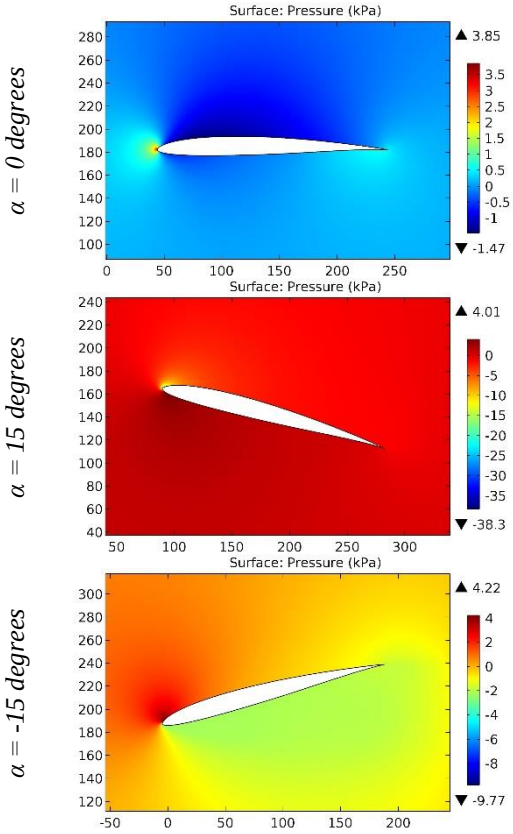

Figure 61. The pressure contours on the surfaces of the HN-216TA airfoil.

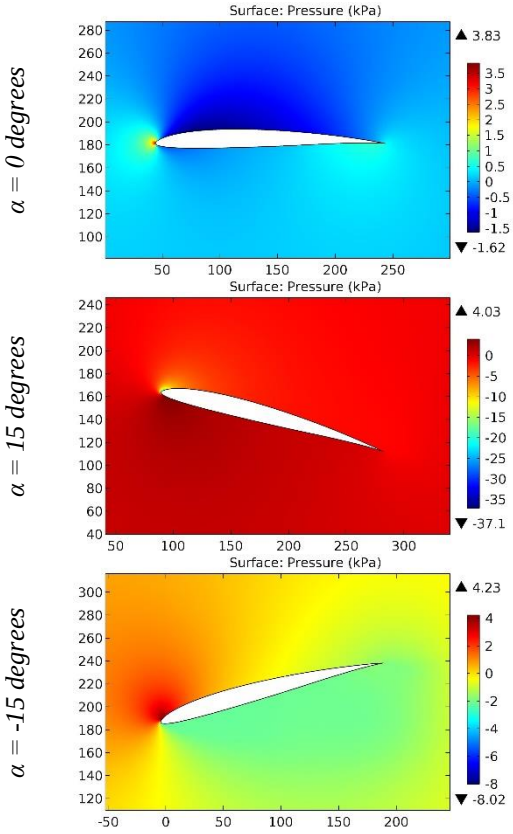

Figure 62. The pressure contours on the surfaces of the HN-217 airfoil.

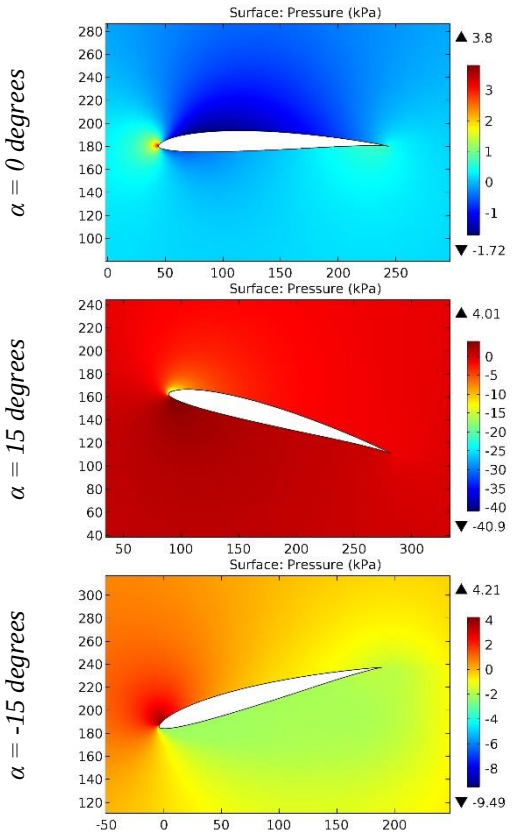

Figure 63. The pressure contours on the surfaces of the HN-227 airfoil.

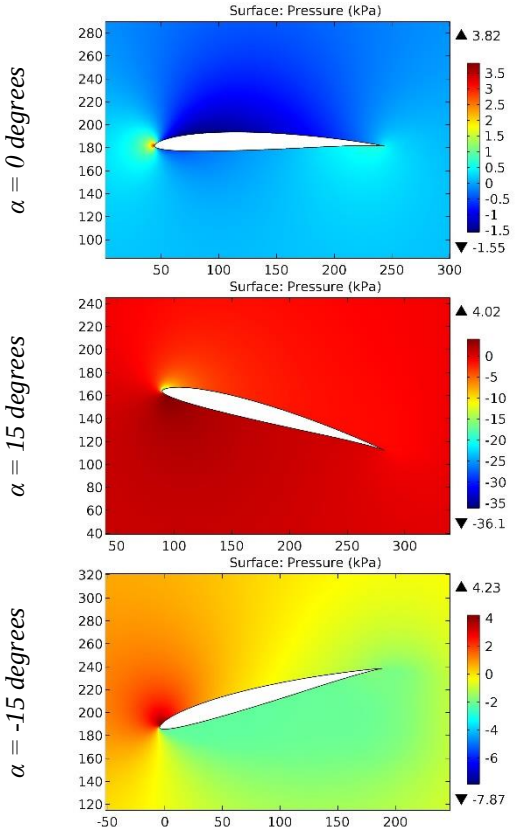

Figure 64. The pressure contours on the surfaces of the HN-239 airfoil.

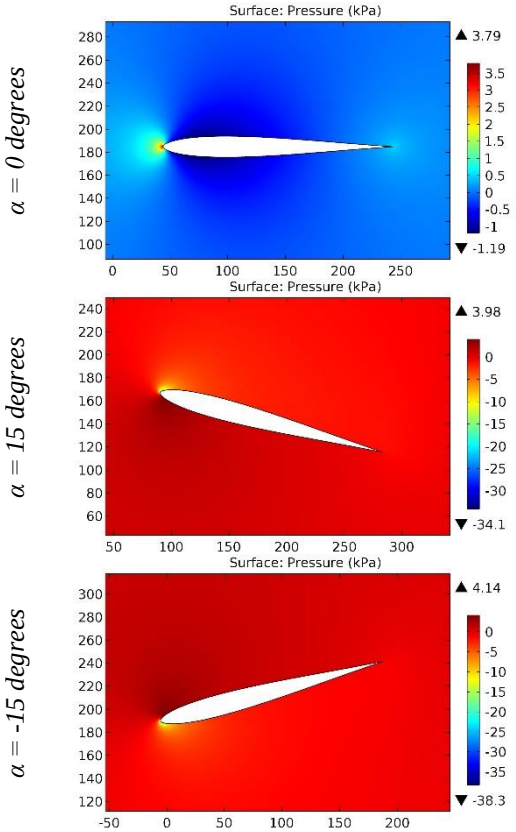

Figure 65. The pressure contours on the surfaces of the HN-274S airfoil.

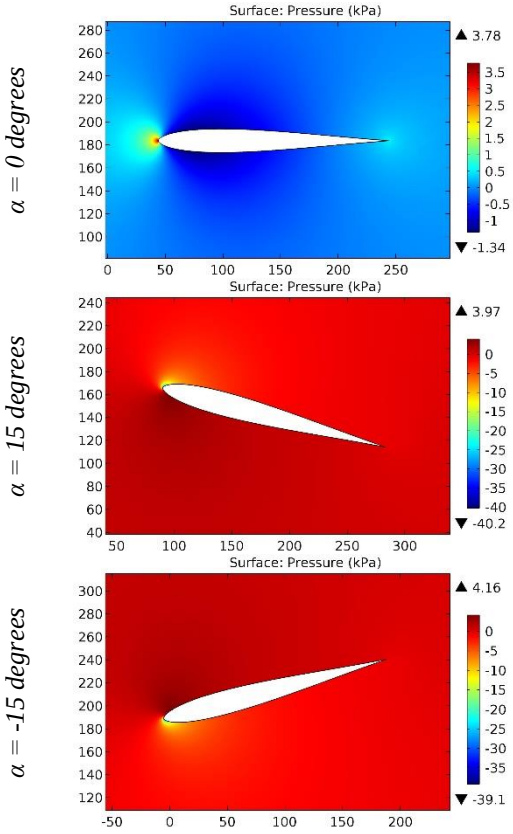

Figure 66. The pressure contours on the surfaces of the HN-275S airfoil.

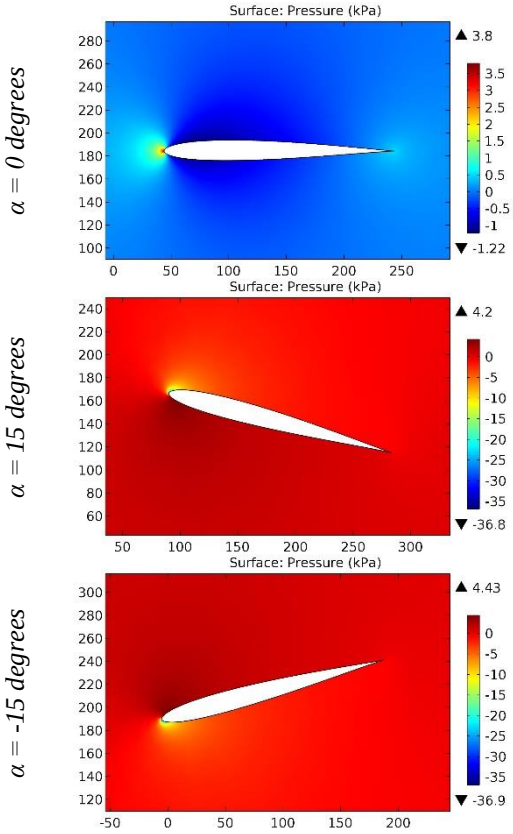

Figure 67. The pressure contours on the surfaces of the HN-276SA airfoil.

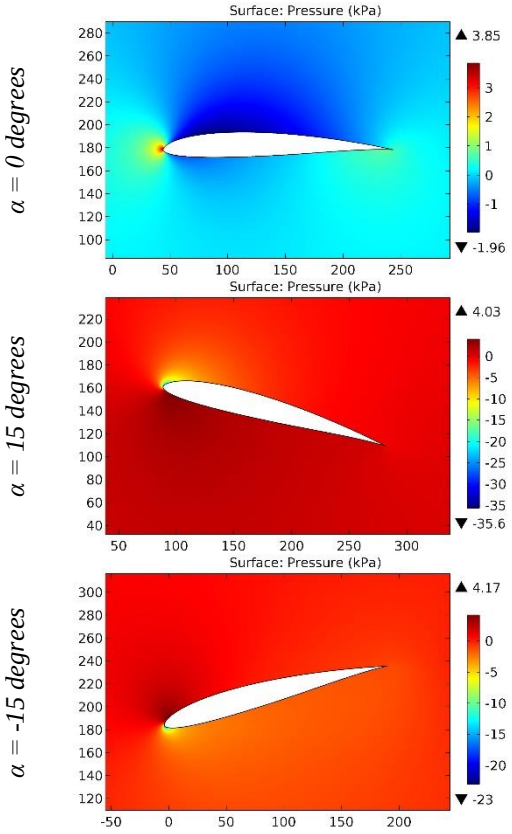

Figure 68. The pressure contours on the surfaces of the HN-304 airfoil.

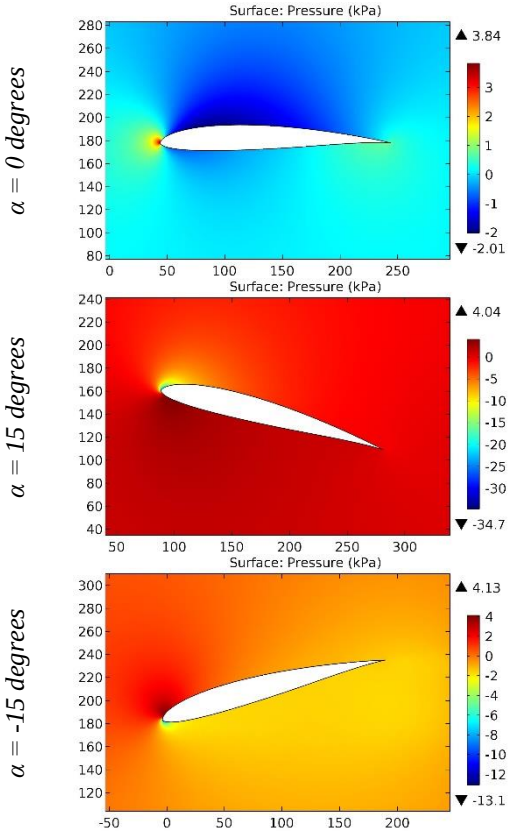

Figure 69. The pressure contours on the surfaces of the HN-304TA airfoil.

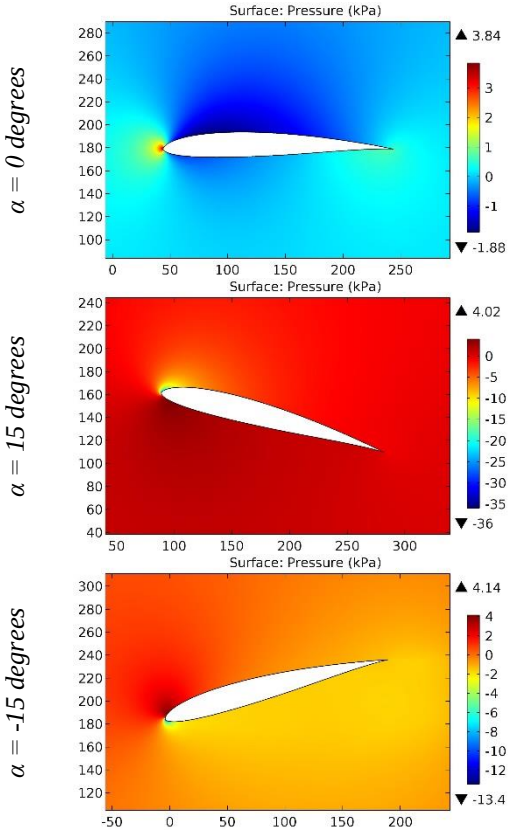

Figure 70. The pressure contours on the surfaces of the HN-309 airfoil.

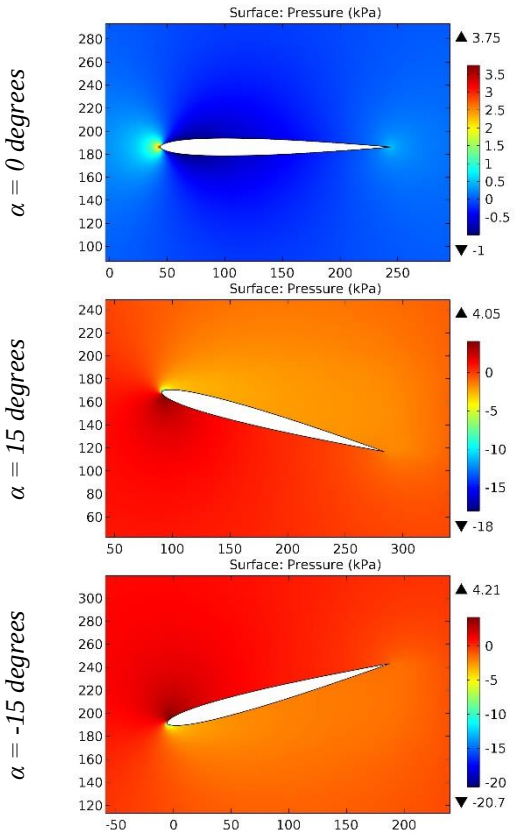

Figure 71. The pressure contours on the surfaces of the HN-311S airfoil.

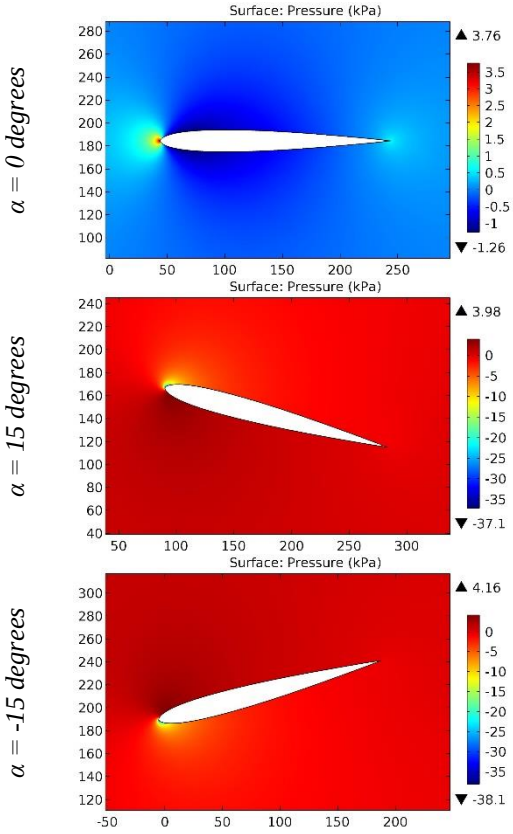

Figure 72. The pressure contours on the surfaces of the HN-312S airfoil.

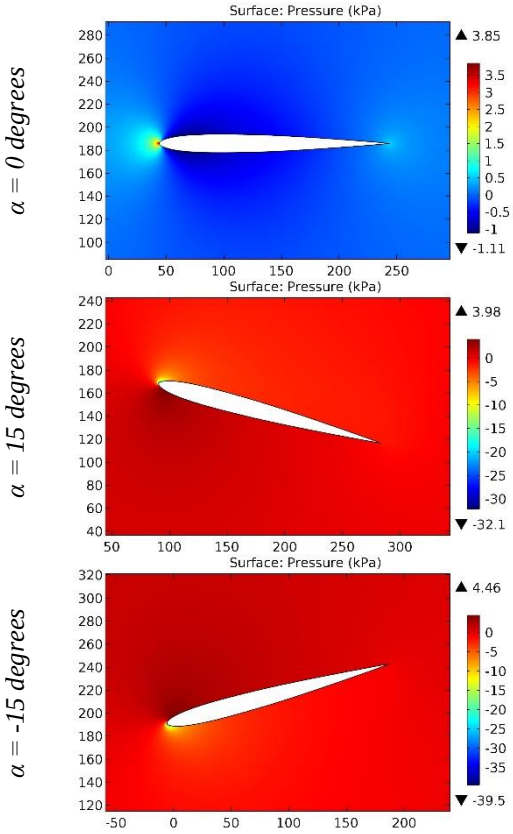

Figure 73. The pressure contours on the surfaces of the HN-315S airfoil.

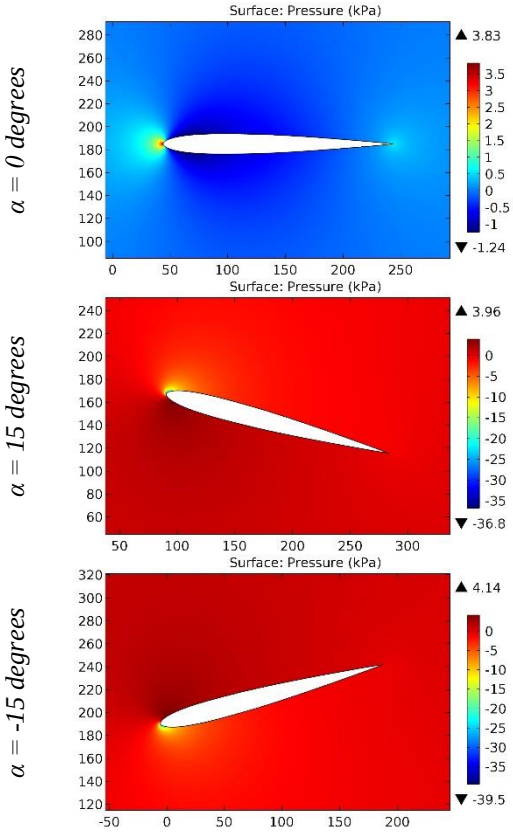

Figure 74. The pressure contours on the surfaces of the HN-316S airfoil.

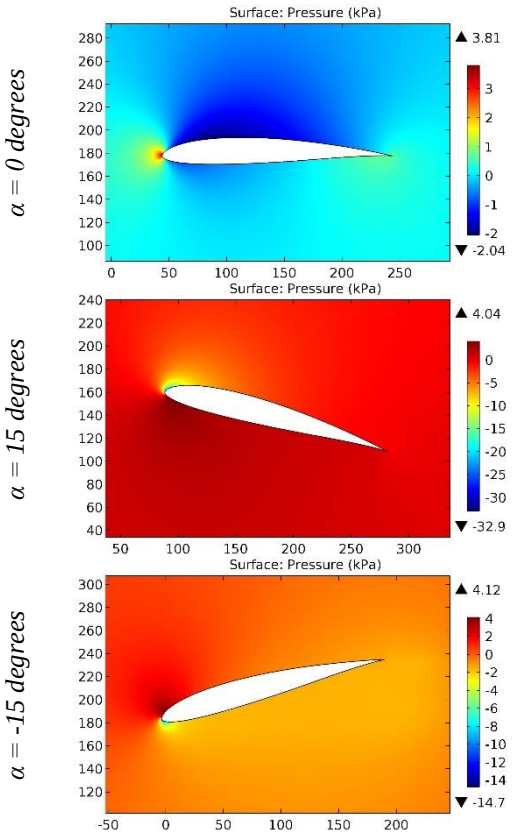

Figure 75. The pressure contours on the surfaces of the HN-319 airfoil.

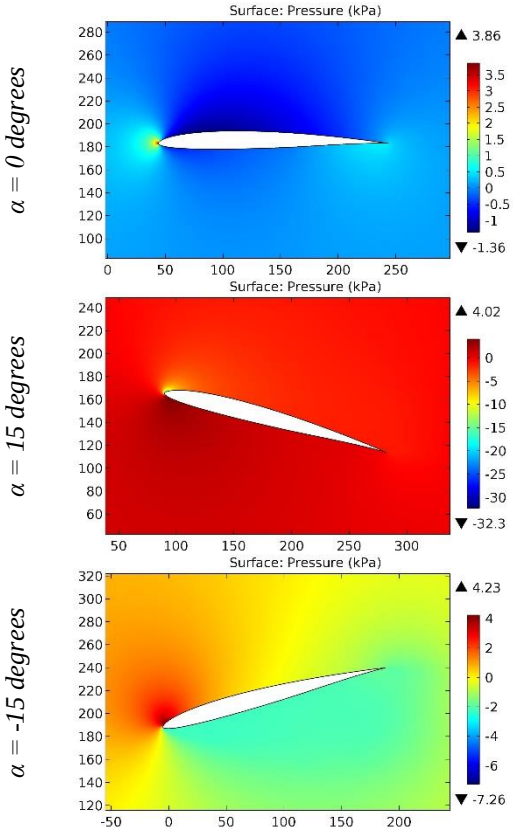

Figure 76. The pressure contours on the surfaces of the HN-321 airfoil.

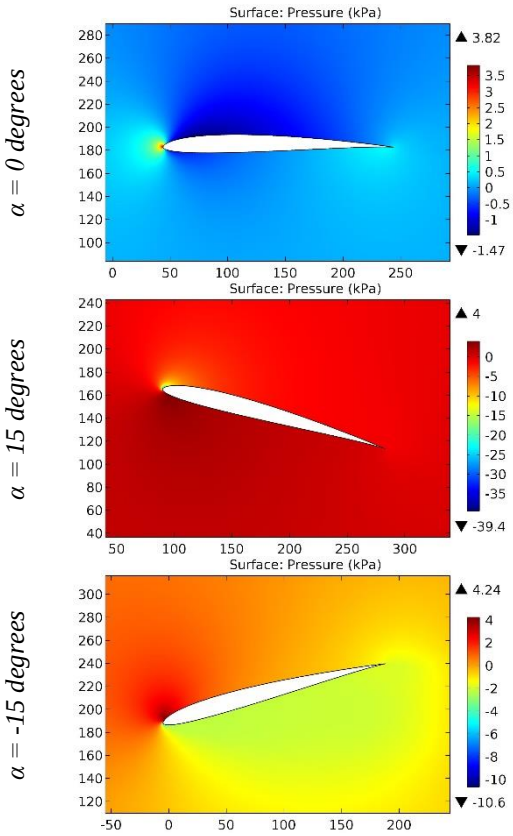

Figure 77. The pressure contours on the surfaces of the HN-326 airfoil.

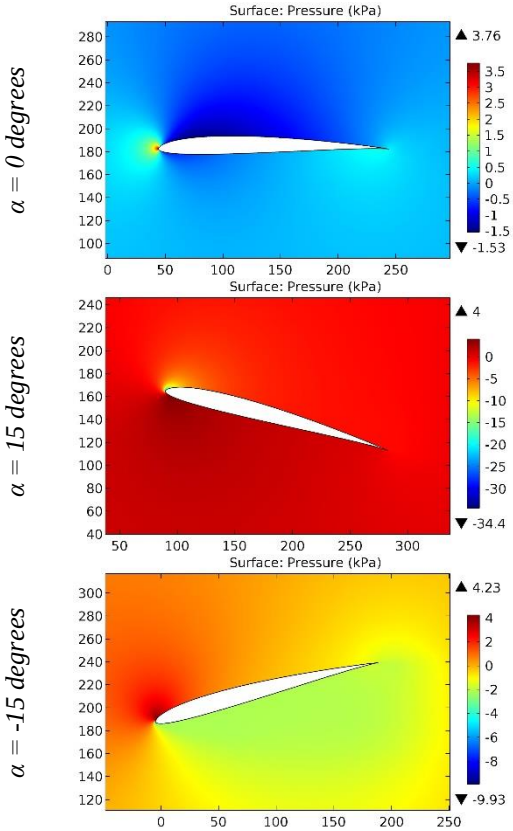

Figure 78. The pressure contours on the surfaces of the HN327 airfoil.

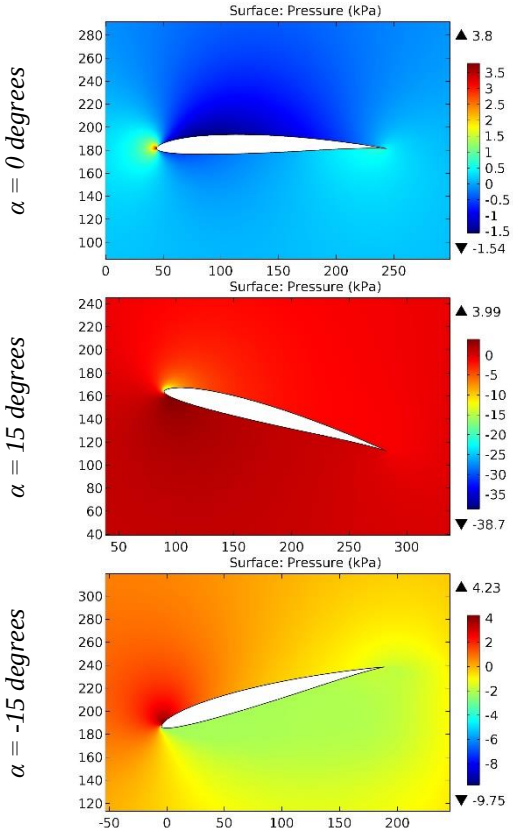

Figure 79. The pressure contours on the surfaces of the HN-333 airfoil.

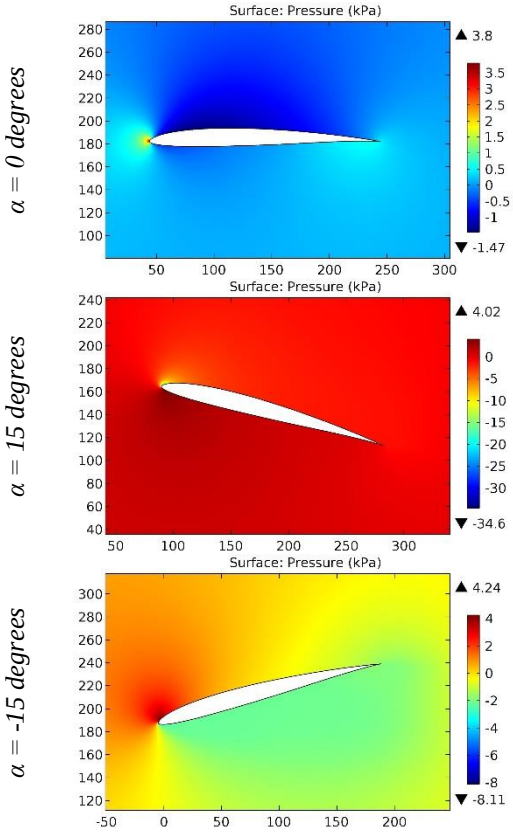

Figure 80. The pressure contours on the surfaces of the HN-350 airfoil.

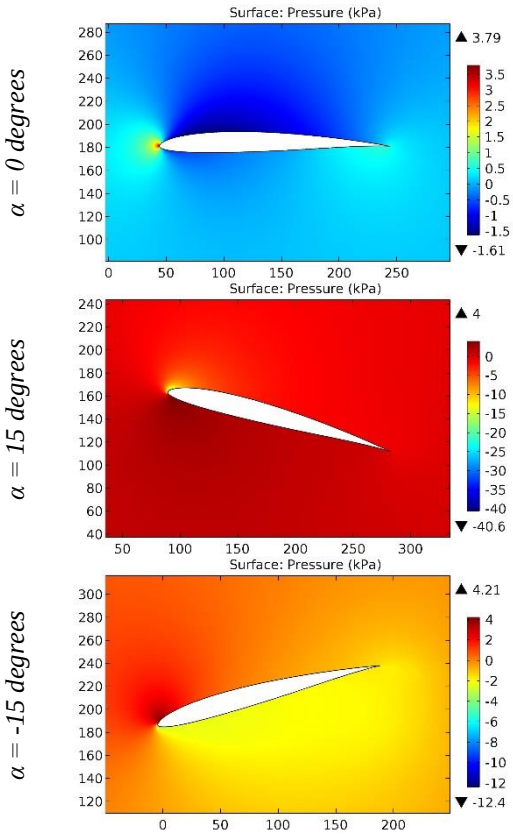

Figure 81. The pressure contours on the surfaces of the HN-350M01 airfoil.

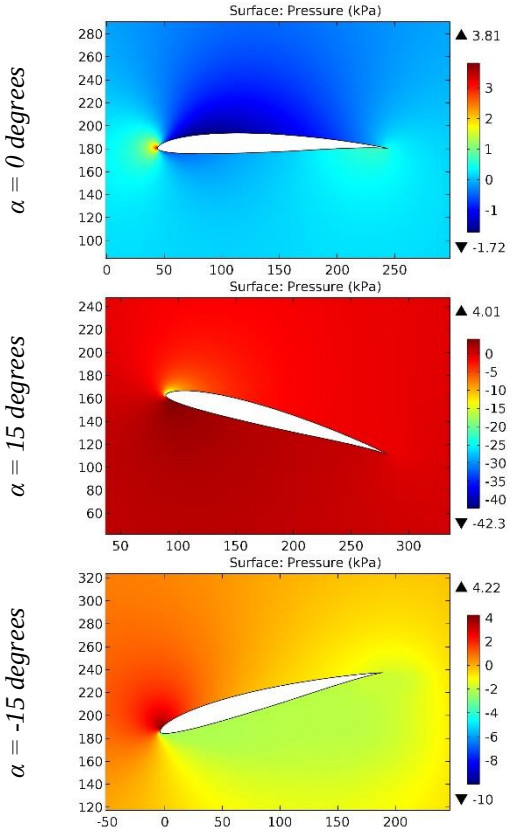

Figure 82. The pressure contours on the surfaces of the HN-350M02 airfoil.

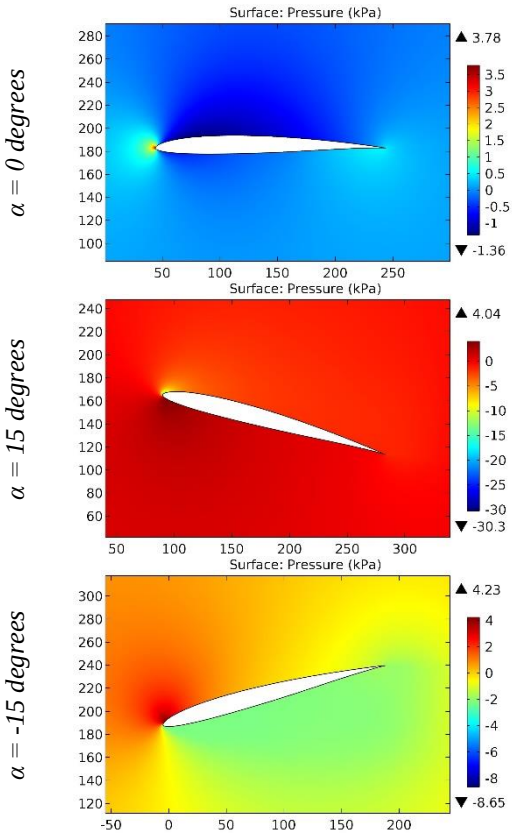

Figure 83. The pressure contours on the surfaces of the HN-352 airfoil.

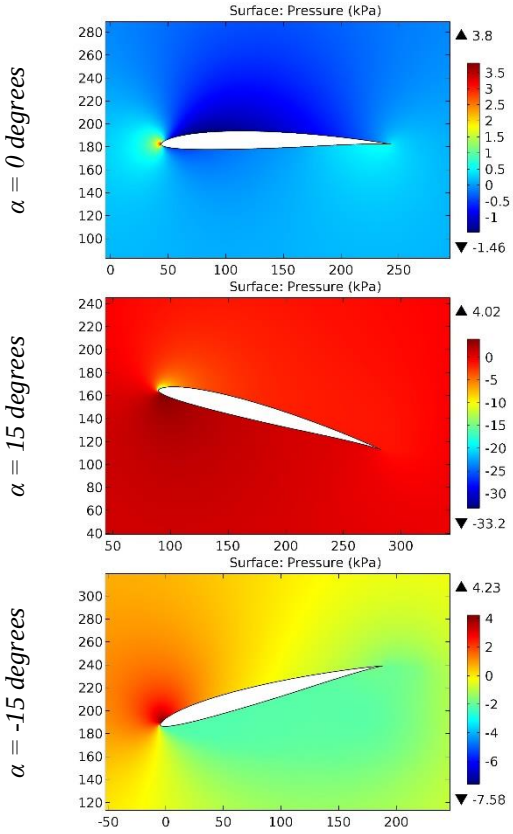

Figure 84. The pressure contours on the surfaces of the HN-354 airfoil.

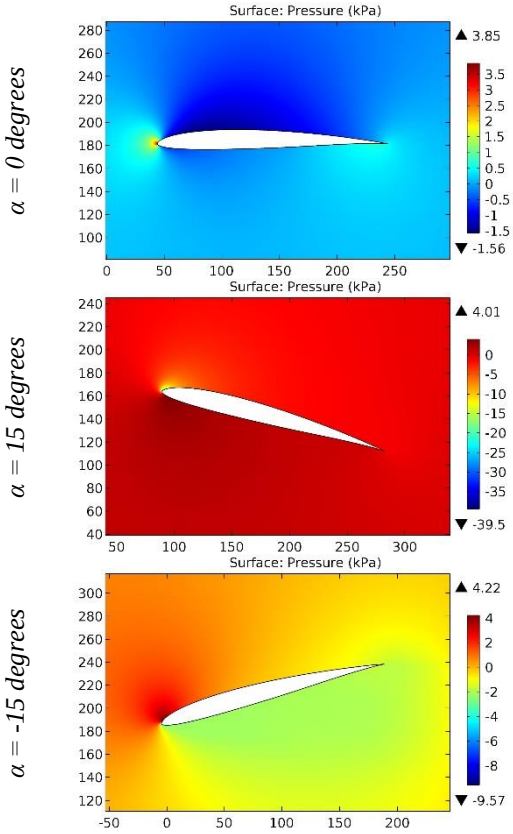

Figure 85. The pressure contours on the surfaces of the HN-354A airfoil.

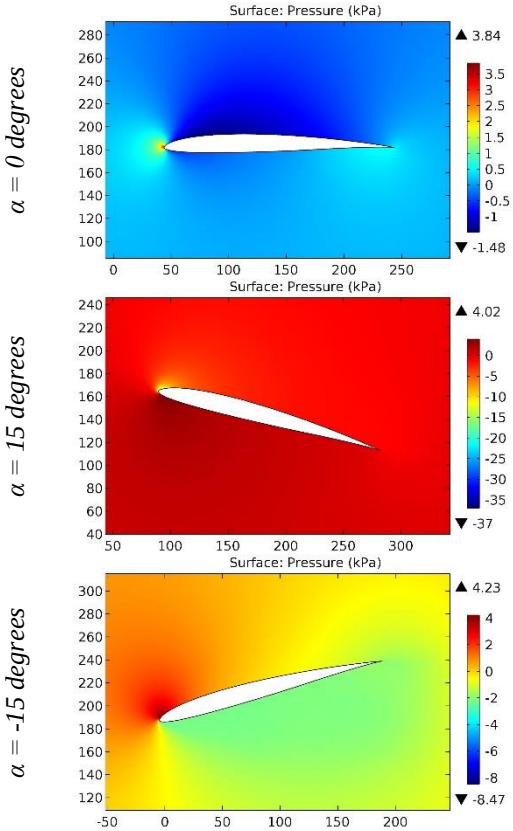

Figure 86. The pressure contours on the surfaces of the HN-354E airfoil.

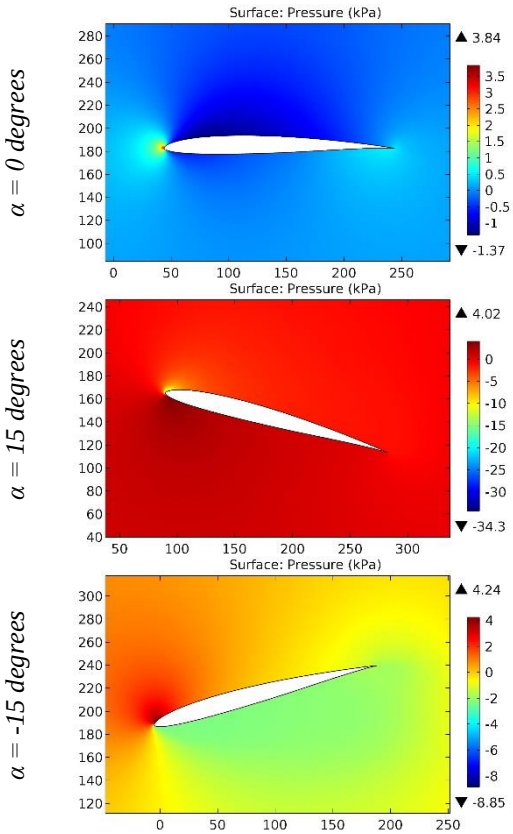

Figure 87. The pressure contours on the surfaces of the HN-354ES airfoil.

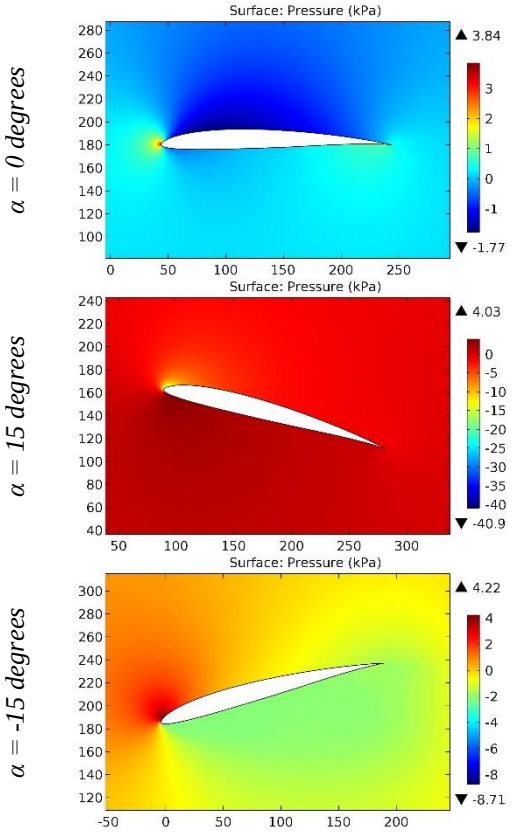

Figure 88. The pressure contours on the surfaces of the HN-354OC airfoil.

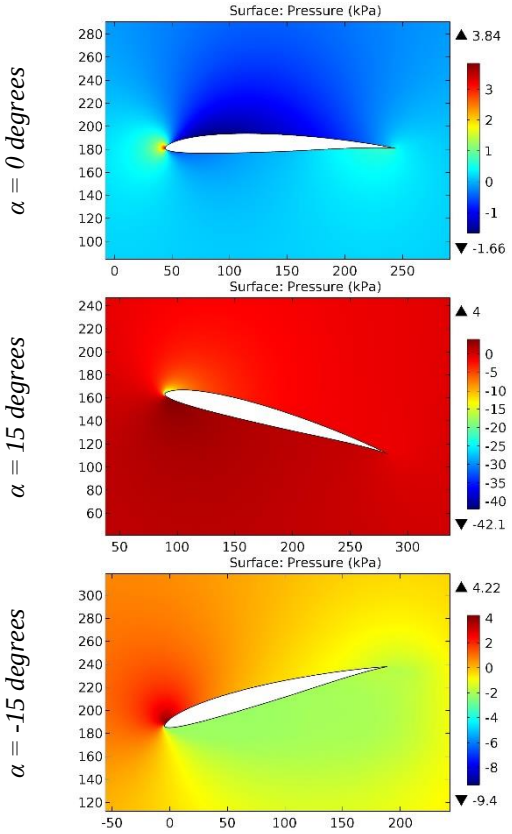

Figure 89. The pressure contours on the surfaces of the HN-354SM airfoil.

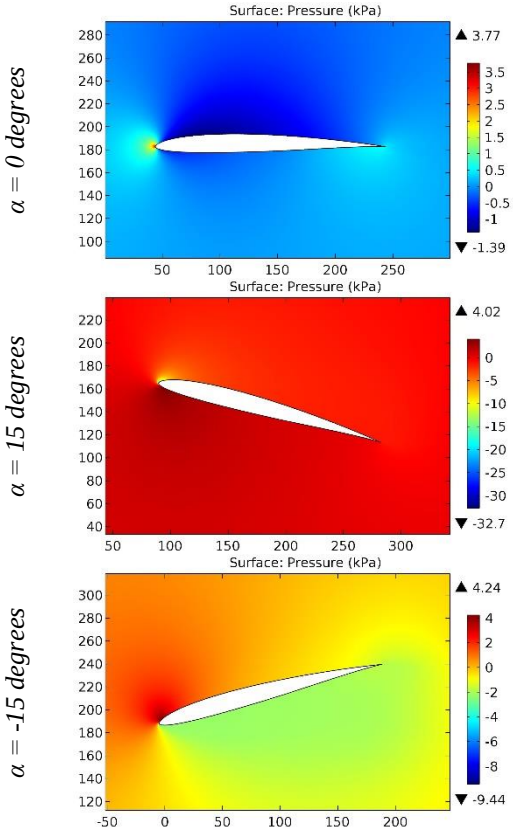

Figure 90. The pressure contours on the surfaces of the HN-354SR airfoil.

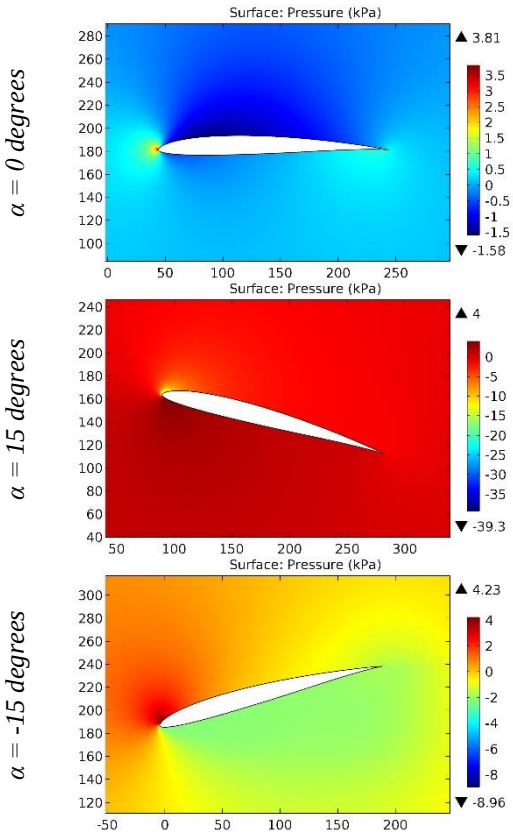

Figure 91. The pressure contours on the surfaces of the HN-360 airfoil.

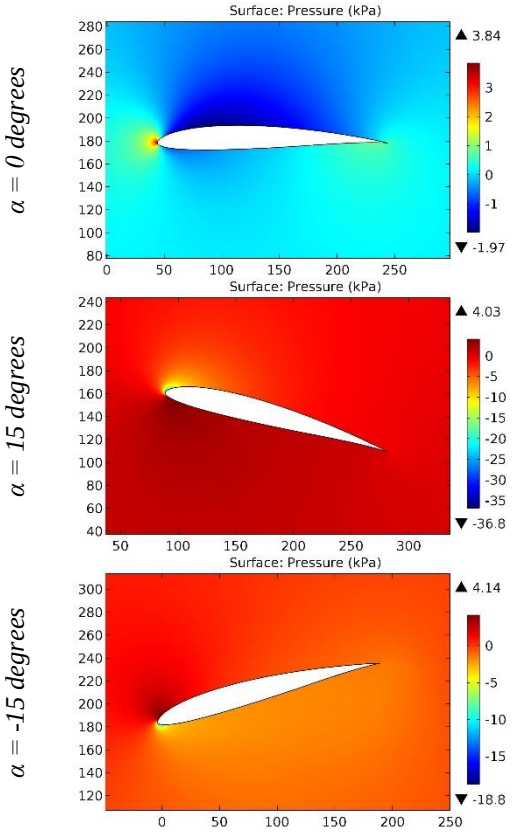

Figure 92. The pressure contours on the surfaces of the HN-409 airfoil.

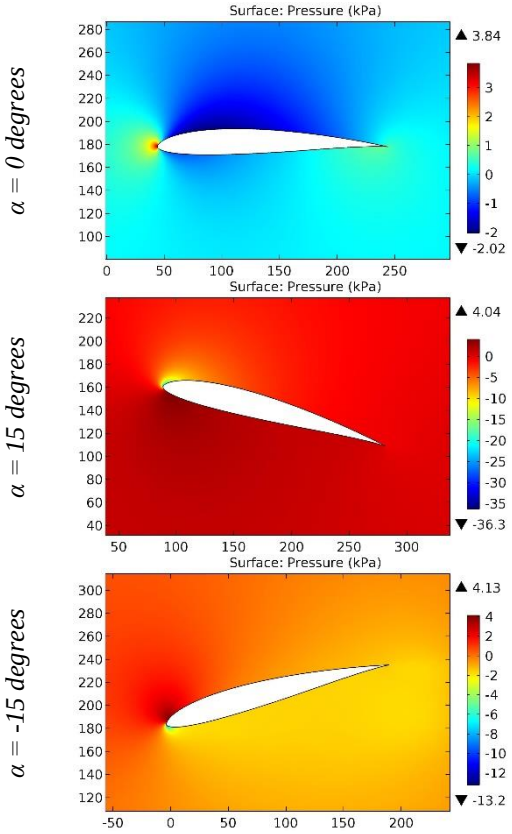

Figure 93. The pressure contours on the surfaces of the HN-411 airfoil.

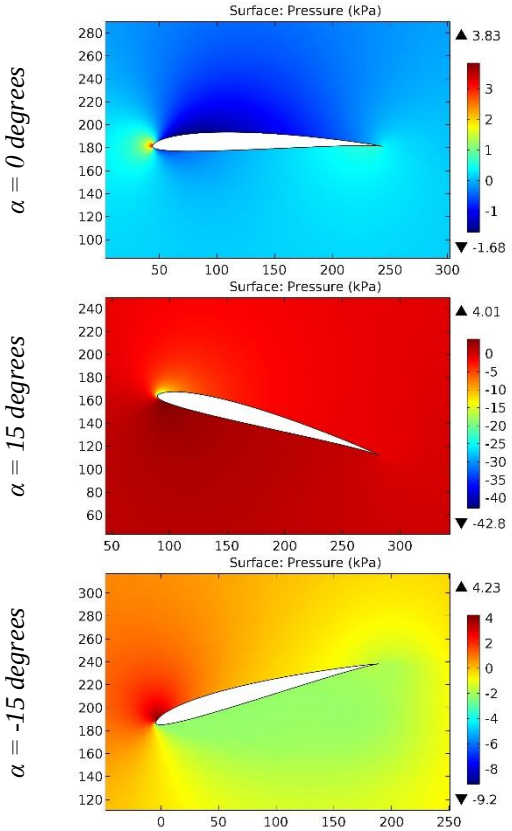

Figure 94. The pressure contours on the surfaces of the HN-417 airfoil.

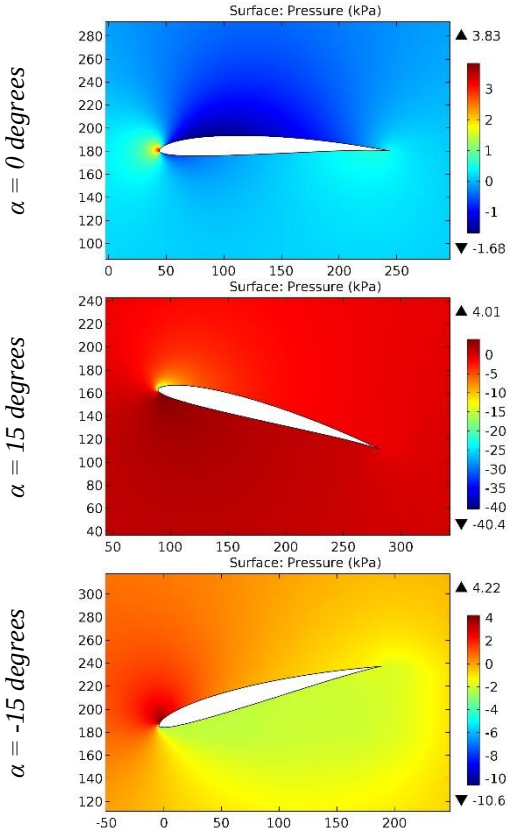

Figure 95. The pressure contours on the surfaces of the HN-418 airfoil.

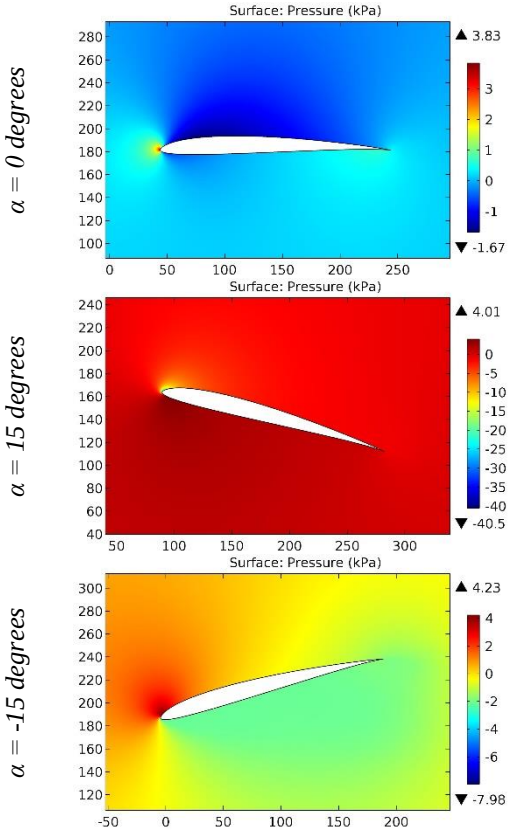

Figure 96. The pressure contours on the surfaces of the HN-419 airfoil.

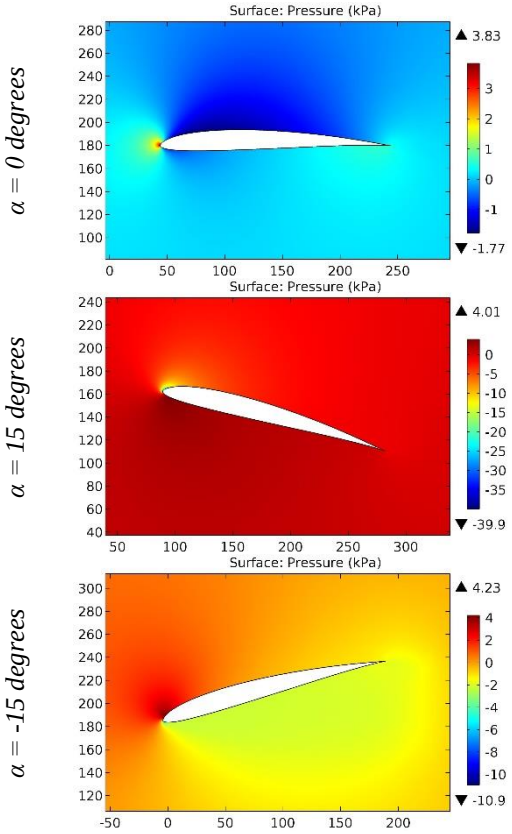

Figure 97. The pressure contours on the surfaces of the HN-424 airfoil.

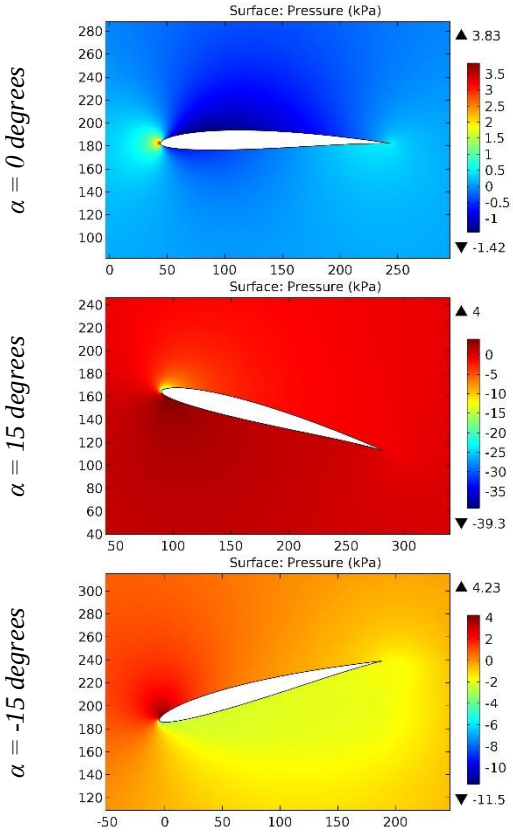

Figure 98. The pressure contours on the surfaces of the HN-436 airfoil.

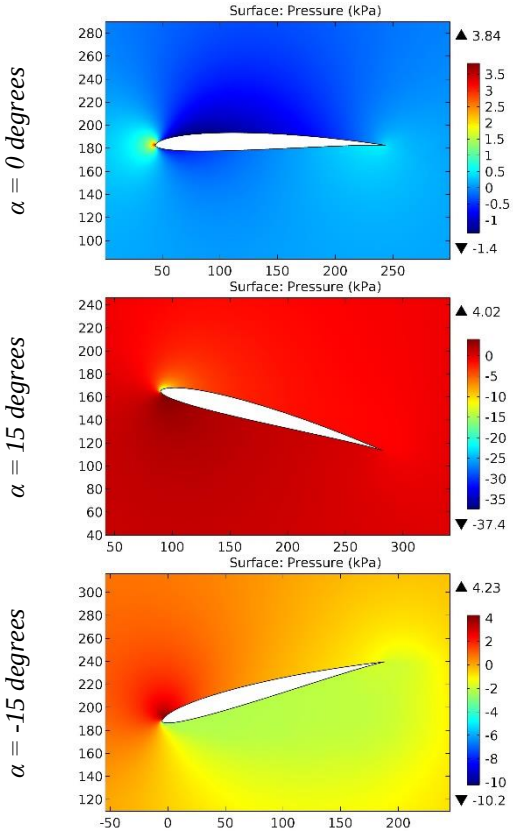

Figure 99. The pressure contours on the surfaces of the HN-446 airfoil.

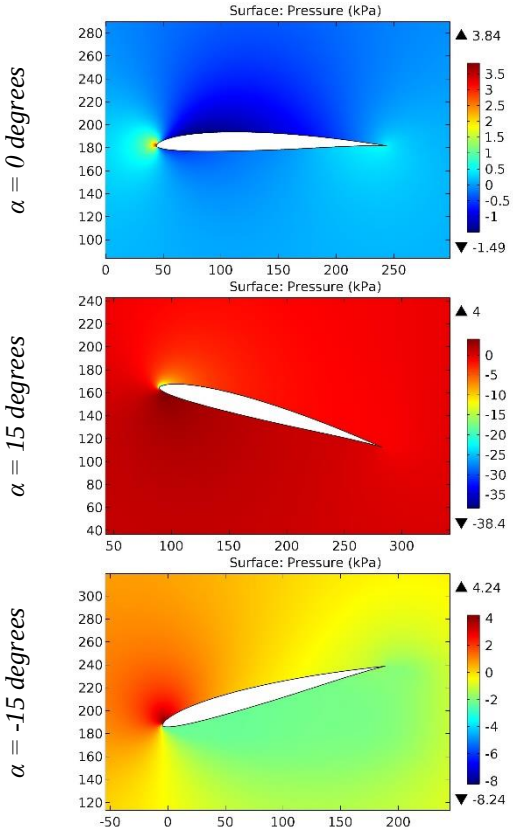

Figure 100. The pressure contours on the surfaces of the HN-450 airfoil.

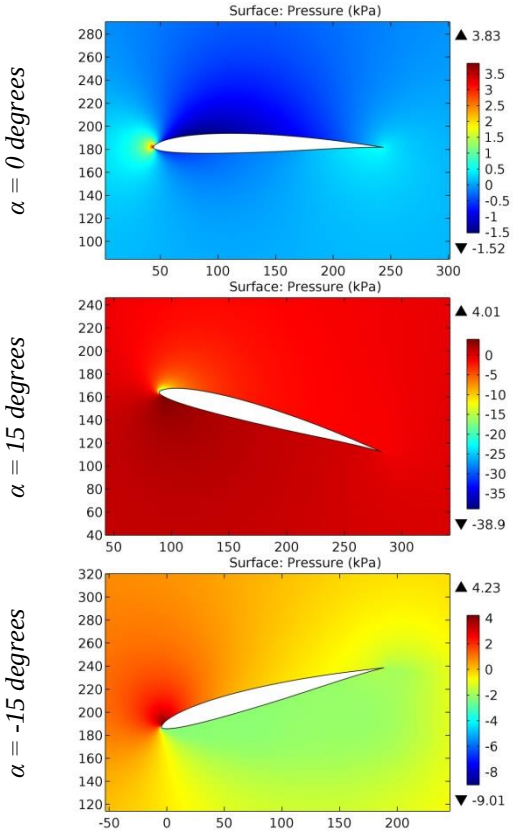

Figure 101. The pressure contours on the surfaces of the HN-450S airfoil.

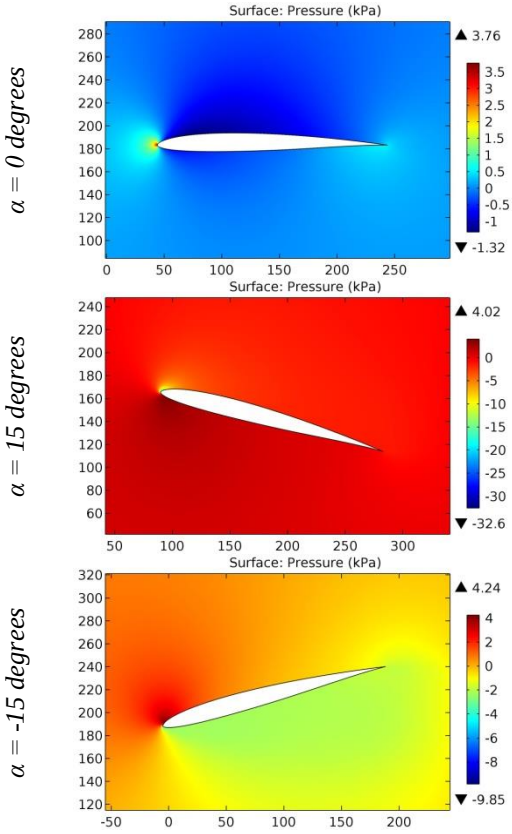

Figure 102. The pressure contours on the surfaces of the HN-462 airfoil.

The maximum increase in pressure on the leading edge occurs at the angle of attack of -15 degrees for the following airfoils: HAR, HAR2, HAR3, HAWKER TEMPEST 37,5% SEMISPAN, HAWKER TEMPEST 61% SEMISPAN, Hill SR 2, HILL-SR2, HL 80-13353, HL813353, HN-003, HN-153S, HN-274S, HN-276SA, HN-311S, HN-312S, HN-315S and HN-316S. The maximum increase in pressure on the leading edge occurs at the angle of attack of 15 degrees for the other airfoils.

Conclusion

The performed analysis of the simulation results showed that the airfoils of the HN series (HN-032, HN-033, HN-034 and further up to HN-462) have the good aerodynamic characteristics, such as the low drag. The large lift force, which affects the aerodynamics of the airplane, is observed when the airplane climb. The following airfoils can be noted that allow you to create the large lift force: H-6355, HANS6407, HAWKER TEMPEST 96,77% SEMISPAN, HN-032, HN-033 and HN-035.

References:

1. Anderson, J. D. (2010). Fundamentals of Aerodynamics. *McGraw-Hill, Fifth edition*.
2. Shevell, R. S. (1989). Fundamentals of Flight. *Prentice Hall, Second edition*.
3. Houghton, E. L., & Carpenter, P. W. (2003). Aerodynamics for Engineering Students. *Fifth edition, Elsevier*.
4. Lan, E. C. T., & Roskam, J. (2003). Airplane Aerodynamics and Performance. *DAR Corp*.
5. Sadraey, M. (2009). Aircraft Performance Analysis. *VDM Verlag Dr. Müller*.
6. Anderson, J. D. (1999). Aircraft Performance and Design. *McGraw-Hill*.
7. Roskam, J. (2007). Airplane Flight Dynamics and Automatic Flight Control, Part I. *DAR Corp*.
8. Etkin, B., & Reid, L. D. (1996). Dynamics of Flight, Stability and Control. *Third Edition, Wiley*.
9. Stevens, B. L., & Lewis, F. L. (2003). Aircraft Control and Simulation. *Second Edition, Wiley*.
10. Chemezov, D., et al. (2021). Pressure distribution on the surfaces of the NACA 0012

airfoil under conditions of changing the angle of attack. *ISJ Theoretical & Applied Science, 09 (101)*, 601-606.

11. Chemezov, D., et al. (2021). Stressed state of surfaces of the NACA 0012 airfoil at high angles of attack. *ISJ Theoretical & Applied Science, 10 (102)*, 601-604.
12. Chemezov, D., et al. (2021). Reference data of pressure distribution on the surfaces of airfoils having the names beginning with the letter A (the first part). *ISJ Theoretical & Applied Science, 10 (102)*, 943-958.
13. Chemezov, D., et al. (2021). Reference data of pressure distribution on the surfaces of airfoils having the names beginning with the letter A (the second part). *ISJ Theoretical & Applied Science, 11 (103)*, 656-675.
14. Chemezov, D., et al. (2021). Reference data of pressure distribution on the surfaces of airfoils having the names beginning with the letter B. *ISJ Theoretical & Applied Science, 11 (103)*, 1001-1076.
15. Chemezov, D., et al. (2021). Reference data of pressure distribution on the surfaces of airfoils having the names beginning with the letter C. *ISJ Theoretical & Applied Science, 12 (104)*, 814-844.
16. Chemezov, D., et al. (2021). Reference data of pressure distribution on the surfaces of airfoils having the names beginning with the letter D. *ISJ Theoretical & Applied Science, 12 (104)*, 1244-1274.
17. Chemezov, D., et al. (2022). Reference data of pressure distribution on the surfaces of airfoils (hydrofoils) having the names beginning with the letter E (the first part). *ISJ Theoretical & Applied Science, 01 (105)*, 501-569.
18. Chemezov, D., et al. (2022). Reference data of pressure distribution on the surfaces of airfoils (hydrofoils) having the names beginning with the letter E (the second part). *ISJ Theoretical & Applied Science, 01 (105)*, 601-671.
19. Chemezov, D., et al. (2022). Reference data of pressure distribution on the surfaces of airfoils having the names beginning with the letter F. *ISJ Theoretical & Applied Science, 02 (106)*, 101-135.
20. Chemezov, D., et al. (2022). Reference data of pressure distribution on the surfaces of airfoils having the names beginning with the letter G (the first part). *ISJ Theoretical & Applied Science, 03 (107)*, 701-784.
21. Chemezov, D., et al. (2022). Reference data of pressure distribution on the surfaces of airfoils having the names beginning with the letter G (the second part). *ISJ Theoretical & Applied Science, 03 (107)*, 901-984.
22. Chemezov, D., et al. (2022). Reference data of pressure distribution on the surfaces of airfoils having the names beginning with the letter G (the third part). *ISJ Theoretical & Applied Science, 04 (108)*, 401-484.